ARTICLE

https://doi.org/10.1038/s41586-018-0859-7

Introns are mediators of cell response to starvation

Julie Parenteau[1], Laurine Maignon[1], Mélodie Berthoumieux[2], Mathieu Catala[1], Vanessa Gagnon[1] & Sherif Abou Elela[1]*

Introns are ubiquitous features of all eukaryotic cells. Introns need to be removed from nascent messenger RNA through the process of splicing to produce functional proteins. Here we show that the physical presence of introns in the genome promotes cell survival under starvation conditions. A systematic deletion set of all known introns in budding yeast genes indicates that, in most cases, cells with an intron deletion are impaired when nutrients are depleted. This effect of introns on growth is not linked to the expression of the host gene, and was reproduced even when translation of the host mRNA was blocked. Transcriptomic and genetic analyses indicate that introns promote resistance to starvation by enhancing the repression of ribosomal protein genes that are downstream of the nutrient–sensing TORC1 and PKA pathways. Our results reveal functions of introns that may help to explain their evolutionary preservation in genes, and uncover regulatory mechanisms of cell adaptations to starvation.

The protein-encoding sequences of most eukaryotic genes are interrupted by intervening non-coding sequences (introns) that need to be removed through the process of splicing[1,2]. The compact genome of the yeast *Saccharomyces cerevisiae* contains only 295 introns, which are located in 280 genes[3–5] (Fig. 1a). Only nine yeast genes contain more than one intron and most introns are shorter than 500 nucleotides[3,6]. In this study, we present what is—to our knowledge—the first complete collection of yeast strains each with a deletion of a specific intron. The analyses of this collection provide direct evidence for global functions of introns that may explain their preservation during evolution, regardless of the function or expression of the host gene of the intron. Phenotypic, transcriptomic and genetic analyses of intron deletion (Δi) strains indicate that introns promote growth under starvation conditions by promoting the repression of ribosomal protein genes (RPGs) in response to the TORC1–PKA pathway. Our work reveals a paradigm of nutrient sensing and adaptation to stationary growth that uses introns as enhancers of gene repression during starvation.

Introns are not essential in rich medium

Most intron-containing genes in yeast are non-essential for growth and participate in a variety of genetic and biochemical pathways (Supplementary Table 1). Only 8 introns contain a small nucleolar RNA, 19 contain hypothetical non-coding RNAs and 20 overlap with an open reading frame (Fig. 1a and Supplementary Table 1). Therefore, the majority of intron deletions should not disrupt essential genes. To understand intron function, we deleted every intron from the yeast genome without leaving a heterologous sequence behind. We created a total of 295 single and 9 double (in cases in which genes carried two introns) Δi strains (Fig. 1b, Extended Data Fig. 1a and Supplementary Table 1). All but five of the Δi strains supported sporulation and growth on rich medium (yeast extract peptone dextrose, YEPD) (Fig. 1b). The effect of these five essential introns on growth is repressed by expressing the allele that lacks the intron from heterologous promoters, or—in one case—by expressing an overlapping gene from a plasmid (data not shown)[7]. The growth rate of the 290 viable Δi strains was determined in YEPD medium; growth was affected by more than 15% in only five Δi strains—*yra1Δi*, *mtr2Δ1i*, *mtr2Δ5i*, *hac1Δi* and *bud25Δi* (Fig. 1b). The defect of these five Δi strains was rescued through expression from alternative promoters, or from the expression of an overlapping gene[7,8]. We therefore conclude that only a minority of introns are required for growth in rich medium, and that the few that are required promote growth by repressing the expression of deleterious genes.

Introns promote resistance to starvation

In nature, yeast often competes for limited nutritional resources[9]. Accordingly, we examined the capacity of all Δi strains that could be distinguished from wild type using PCR (244 out of 290 deletion strains) to compete with an unmutated strain under starvation conditions. Cells were grown in 3 communities, each of which contained 1 wild type and 94 Δi strains, and their relative abundance in the culture was measured as nutrients were depleted and cells starved (Fig. 1c). Cultures were incubated for six days after reaching the stationary phase in minimal medium (medium contains the minimum amount of nutrients required for growth) and the ratio of the strains to one another was determined using PCR specific to intron deletion (Fig. 1c and Extended Data Fig. 1b). The majority of the Δi strains (64%) disappeared from cultures during stationary phase, whereas they outcompeted the wild-type strain when nutrients were added to the starving culture (Fig. 1d). The effect of introns on growth was not linked to host-gene function (Fig. 1e). Overall, the data indicate that although introns may negatively regulate growth in rich medium, they are required for cell maintenance under starvation conditions regardless of host-gene function.

Introns foster growth in stationary phase

To better characterize the effect of introns on cell growth under starvation conditions, the wild-type and Δi-strain cell mix was grown in medium that was low in phosphate or glucose and the survival of Δi strains was assayed after 150 doublings of the population (Fig. 2a). Notably, 80% or 90% of the Δi strains were under-represented or lost from the culture in low-glucose or low-phosphate conditions, respectively (Fig. 2b). Overall, 94% of the Δi strains affected growth when either phosphate or glucose were limiting, regardless of host-gene

[1]RNA Group, Département de Microbiologie et d'Infectiologie, Faculté de Médecine et des Sciences de la Santé, Université de Sherbrooke, Sherbrooke, Quebec, Canada. [2]RNA Group, Département de Biochimie, Faculté de Médecine et des Sciences de la Santé, Université de Sherbrooke, Sherbrooke, Quebec, Canada. *e-mail: Sherif.Abou.Elela@USherbrooke.ca

© 2019 Springer Nature Limited. All rights reserved.

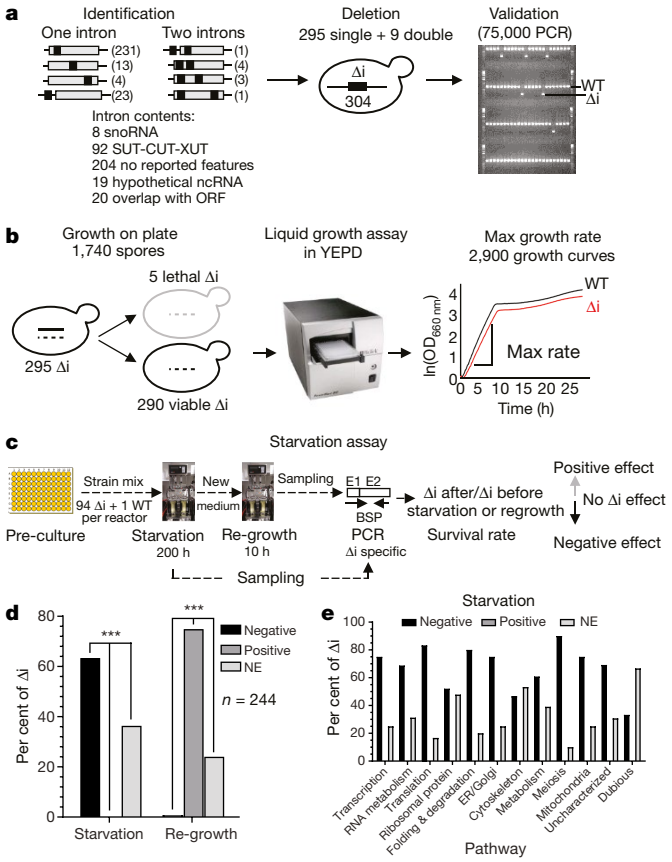

Fig. 1 | Introns are required for cell survival under starvation conditions. a, Description and deletion strategy for yeast introns. Black and grey boxes indicate introns and exons, respectively. Lines indicate UTRs. The numbers of genes that contain introns at different positions are indicated in parentheses. Features found in introns are indicated beneath. Introns were deleted using homologous recombination and Δi strains were selected using PCR. **b**, The diploid Δi strains were dissected and tested for growth in liquid medium to calculate the maximum growth rate. **c**, Δi strains were pre-cultured individually, and then tested for competitive growth over a period of 200 h. The Δi strains ($n = 244$ biologically independent strains) were detected using deletion-specific PCR primers. The survival rate was calculated as the ratio of Δi to wild-type (WT) strains at the beginning and the end of the culture period. High and low survival rates indicate intron deletion that has a positive and negative effect, respectively, on cell growth. **d**, Per cent of Δi strains with positive, negative or no effect (NE) on growth after starvation or after re-growth in fresh medium, compared using χ^2 test. $^{***}P < 4 \times 10^{-9}$. **e**, Histogram summarizing the effect of intron deletion in different metabolic pathways on cell survival. BSP, boundary-spanning primers; CUT, cryptic unstable transcript; E1, exon 1; E2, exon 2; ORF, open reading frame; ncRNA, non-coding RNA; snoRNA, small nucleolar RNA; SUT, stable uncharacterized transcript; XUT, Xrn1-sensitive unstable transcript.

function (Fig. 2c). The growth profiles of individual Δi strains indicate that their disappearance from the cultures is due to reduced growth during stationary phase. Most Δi strains grew in a manner similar to the wild type in the exponential phase of growth, but stopped growing shortly after the pre-stationary phase regardless of the host-gene function (Fig. 2d and Extended Data Fig. 2). In a few cases (such as *TEF4Δi* and *YOS1Δ1i*), the Δi-strain cells entered the stationary phase much earlier or at a lower density than did the wild-type cells (Extended Data Fig. 2a, f). We conclude that introns are specifically required for growth in the stationary phase of the culture when nutrients are depleted.

Expression-independent intron functions

Examining the effect of intron deletion on the abundance of the host mRNA in different phases of growth revealed no association between the abundance of the host mRNA and the effect of the intron on growth (Fig. 3a). Consistently, intron deletion did not have a uniform effect on the response of the host gene to starvation (Fig. 3b and Extended Data Fig. 2). By contrast, entry into the stationary phase increased the abundance of introns, which suggests that there is a link between nutrient depletion and the accumulation of unspliced RNA (Fig. 3c). This suggests that the ultimate effect of introns on cell physiology is linked to changes in the abundance of introns, and is not due to specific changes in the expression pattern of host genes.

RNA sequencing indicated that half of yeast introns accumulate and/or are under-spliced in the stationary phase of growth (Extended Data Fig. 3a). This repression of splicing was mostly intron-dependent (Extended Data Fig. 3c, d). Removing the *MMS2* or *YSF3* introns altered the splicing pattern of about 10% of the spliced genes, and induced the expression of highly expressed RPGs (such as those encoding Rpl28p and Rpl30p) in saturated cultures (Extended Data Fig. 3b–d and Supplementary Table 2). This indicates that intron deletion affects growth by altering the splicing equilibrium, which leads to de-repression of RPGs that are normally repressed during starvation. Consistently, inactivation of the temperature-sensitive alleles of the splicing factors Prp4 and Prp11[10] repressed the intron-deletion phenotype (Extended Data Fig. 3e). Inhibiting the expression of RPGs via *IFH1* also repressed the effects of intron deletion (Extended Data Fig. 3e). We conclude that the effect of intron deletion on growth is mediated, at least in part, by changes in the splicing of RPGs.

Transforming the Δi strains with single-copy plasmids (*CEN6* and *ARSH4*) that carry non-sense mutations rescued the intron-deletion phenotype, whereas using an empty plasmid or a plasmid that carries the unmutated gene did not (Fig. 3d and Extended Data Fig. 4a, b). The mutated plasmid produced more unspliced introns than did the unmutated version, which explains the difference in their ability to complement the intron-deletion phenotype (Extended Data Fig. 4c, d). Consistently, increasing the abundance of the cDNA of the host gene did not affect growth (Extended Data Fig. 4e). By contrast, increasing the number of introns regardless of host-gene translation had a negative effect on cell resistance to starvation (Extended Data Fig. 4f). These data are consistent with the notion that introns affect growth through changing the splicing equilibrium, as previously suggested[10]. Together, these results confirm that it is the intron—rather than the protein encoded by the host gene—that is required for cell maintenance during the stationary phase.

Transforming cells that contain the *ysf3Δi* allele with a plasmid that carries the *MMS2* gene containing a stop codon, and vice versa, rescues the growth defect (Fig. 3e). This cross complementation is not restricted to *YSF3* and *MMS2*: it was observed with all the tested introns that affect growth, regardless of the function and expression pattern of the host gene (Fig. 3b, f). By contrast, plasmids that express introns that do not affect growth under starvation (such as that of the gene *TUB1*) did not alter cell growth or rescue the deletion phenotype (Extended Data Fig. 5a–d). Deletions of more than one intron in the same strain were genetically epistatic, which indicates that introns affect cell growth using the same metabolic pathway (Extended Data Fig. 5e, f). We conclude that introns have a common function required for cell growth under starvation conditions, independent of the expression of their host genes.

Intron function requires 5′ untranslated region

Mutation of the branch point that blocks splicing but permits association with early splicing factors rescued the intron-deletion phenotype, which indicates that the release of the introns is not required for function (Fig. 4a and Extended Data Fig. 4c, d). Expressing the intron out of its gene context, by using a heterologous splicing reporter or substituting one intron with another, did not rescue the deletion phenotype (Extended Data Fig. 6a–c). A plasmid that carries a stop codon and a substitution of the 3′ untranslated region (UTR) of the *MMS2* gene with the *ADH1* terminator sequence or a substitution of exon 2 of *MMS2* with that of *YSF3* or *TUB1* rescued the intron-deletion phenotype,

© 2019 Springer Nature Limited. All rights reserved.

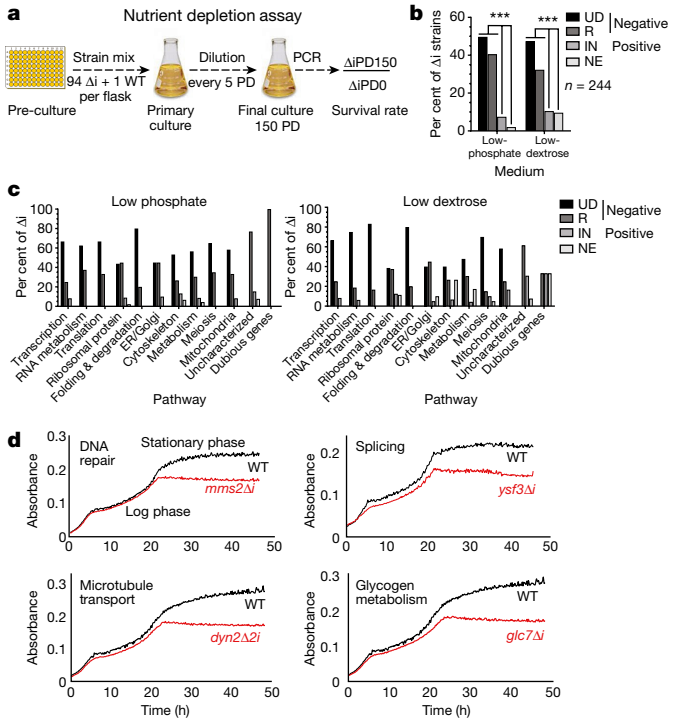

Fig. 2 | Intron deletions repress cell growth by promoting entry into the stationary phase. a, A mixture of Δi and wild-type strains was grown in low-phosphate or low-dextrose medium, and the culture was diluted in the same medium every five doublings. Strains were detected by PCR as described in Fig. 1c. **b**, A descriptive summary of the capacity of Δi strains ($n = 244$ biologically independent strains) to compete for growth in low-phosphate or low-dextrose medium. The presence of the Δi strain in the culture was classified as no effect, undetected (UD), reduced (R) or increased (IN). The χ^2 test was used to compare positive and negative effects. $***P < 2.2 \times 10^{-16}$. **c**, Effect of intron deletion in different metabolic pathways on cell survival in low-phosphate and low-dextrose medium. **d**, Introns promote cell entry into the stationary phase. The mean growth curve of three spores and two technical replicates obtained using quasi-continuous monitoring of optical density in low-dextrose medium. Host-gene function is indicated in the top left. PD, population doubling.

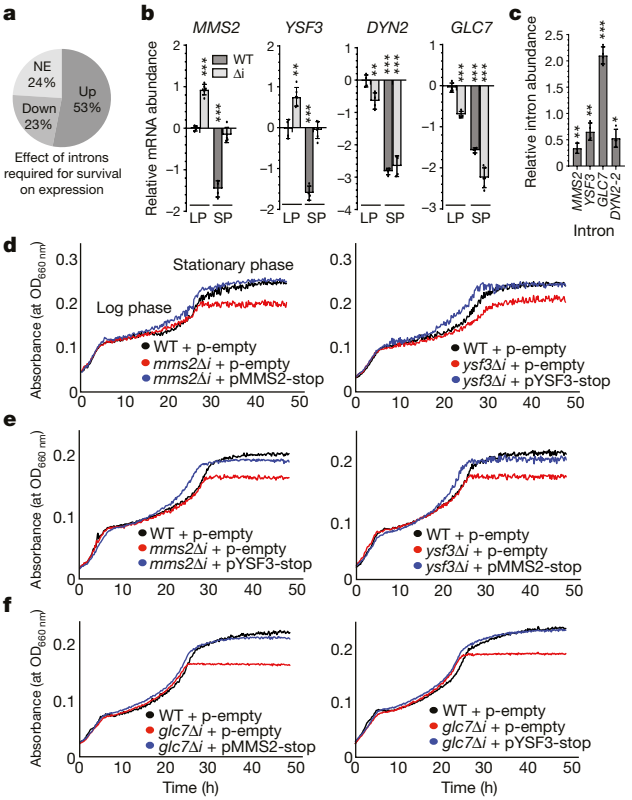

Fig. 3 | Introns promote cell survival independently of host-gene expression. a, Percentage of Δi strains that have increased (up), decreased (down) or no effect on expression. **b**, The abundance of the host mRNA was determined in log phase (LP) and stationary phase (SP) in the presence or absence of introns using quantitative PCR with reverse transcription (RT–qPCR). Relative mRNA abundance given as $\log_2$(mRNA abundance of the gene in each condition/mRNA abundance of the gene in wild-type LP). Bars represent mean ± s.d. from two (wild type and *dyn2Δ2i*) or three (*mms2Δi*, *ysf3Δi* and *glc7Δi*) biologically independent strains. The difference between conditions was calculated relative to wild-type log phase, using a two-sided *t*-test and assuming unequal variances. $*P < 0.05$, $**P < 0.01$, $***P < 0.001$. **c**, Intron abundance in wild-type cells was determined in the log phase and stationary phase of growth using RT–qPCR. Bars and *P* values were calculated as in **b**. Relative intron abundance is given as $\log_2$(intron abundance of the gene in wild-type SP/intron abundance of the gene in wild-type LP). **d**, Cells that lack introns were transformed with plasmids that express genes carrying a stop codon (pMMS2-stop or pYSF3-stop), and compared to strains that carry empty plasmids (p-empty). **e**, Cells that lack one intron were transformed with plasmids that express the intron of a different gene, and compared to wild-type and Δi strains. **f**, Cells that lack the intron of the *GLC7* gene (*glc7Δi*), which does not affect the host-gene response to starvation, were transformed with the pMMS2-stop and pYSF3-stop plasmids. For growth, the mean curve of nine (**d**, **e**) or six (**f**) different clones and two technical replicates is shown.

whereas substitution of the promoter and 5′-UTR sequence with that of *ACT1* did not (Fig. 4b and Extended Data Fig. 6d–f). Substitution of the first half of the intron sequence with that of the *ACT1* intron (hereafter referred to as 'SWAP1') did not rescue the intron-deletion phenotype, whereas the substitution of the second half of the sequence (hereafter referred to as 'SWAP2') partially restored growth (Fig. 4c). These data emphasize the importance of the sequence that surrounds the 5′-end of the intron, and explain why it is that introns do not support growth outside the context of their host gene.

The predicted structure of introns that affect growth under starvation conditions features base-pairing between the intron and the 5′-UTR sequence, whereas the predicted structure of introns that have no effect on growth does not (Extended Data Fig. 7a, b). The structure that forms between the 5′ UTR and the intron often involved the 5′ splice site and/or the branch point, and the effect of mutations on growth correlated with the degree of change in the structure of the 5′ end of the intron (for example, SWAP1 and SWAP2; Fig. 4c and Extended Data Fig. 7c). Two-nucleotide substitutions that destabilized the interaction between the 5′ UTR and the intron (that is, unfolded the structure) failed to rescue the intron-deletion phenotype, whereas those that restored the structure (that is, refolded the structure) did (Fig. 4d, e and Extended Data Fig. 7d). Disrupting the structure of the 5′ UTR and intron in an otherwise-unmutated chromosomal copy of the *MMS2* gene reproduced the intron-deletion phenotype, whereas restoring the structure mimicked wild-type growth (Fig. 4f). These results explain how the gene context may influence intron function, and suggest that the 5′ UTR may contribute to the structure and function of introns.

Sequencing the transcriptome of cells in different phases of growth identified 1,397 induced and 1,468 repressed genes during the stationary phase (Supplementary Table 3 and Extended Data Fig. 8a). Genes that are associated with stationary growth—such as *SNZ1* and *SSA3*—were upregulated, which confirms the growth status of the cells (Supplementary Table 3). Deleting the introns from genes with different functions (such as the chromatin-remodelling *MMS2* or the splicing regulator *YSF3*) altered the expression of a common set of genes in the stationary phase of growth (Fig. 5a, b and Supplementary Table 4). Expression of only seven genes varied significantly (adjusted $P < 0.001$ (*t*-test, one-sided), as described in Methods) between these

© 2019 Springer Nature Limited. All rights reserved.

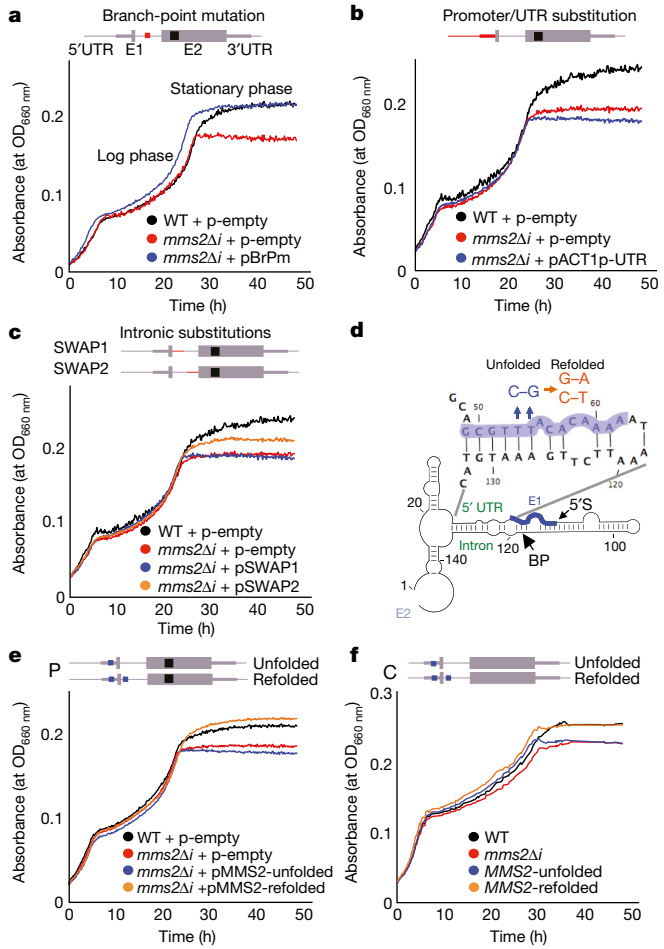

Fig. 4 | The 5′ UTR is required for intron functions. a, A plasmid that expresses a copy of the *MMS2* gene carrying both stop-codon and branch-point mutations (top) was transformed in Δi strains. Stop-codon mutation is shown as a black box. **b**, The effect of plasmids that express a *MMS2* ORF carrying a stop-codon mutation from the *ACT1* promoter (labelled 'pACT1p-UTR') on growth was examined. **c**, The sequence of the 5′ (pSWAP1) or 3′ (pSWAP2) ends of the intron was substituted with a sequence of equal length in the plasmid carrying the stop codon, and the effect on growth was examined. **d**, The secondary structure surrounding the 5′ end of the *MMS2* intron was determined as described in Methods. Mutations that disrupt the interaction with the UTR are shown in blue, and those that restore this interaction are shown in orange. **e**, Growth curves of *mms2*Δ*i* cells transformed with plasmids that carry a stop-codon and mutations that disrupt the intron–5′ UTR structure (unfolded) or restore this structure (refolded). **f**, Mutations in the 5′ UTR that disrupt the interaction with the intron (unfolded) and mutations in the intron that restore the interaction (refolded) were introduced in the unmutated chromosomal copy of *MMS2*, and tested for growth. The experiments were repeated independently six (**a**, **b**, **c**, **e**) or three (**f**) times with similar results. BP, branch point; pBrPM, plasmid containing branch-point mutation in *MMS2* stop codon; p-empty, empty plasmid.

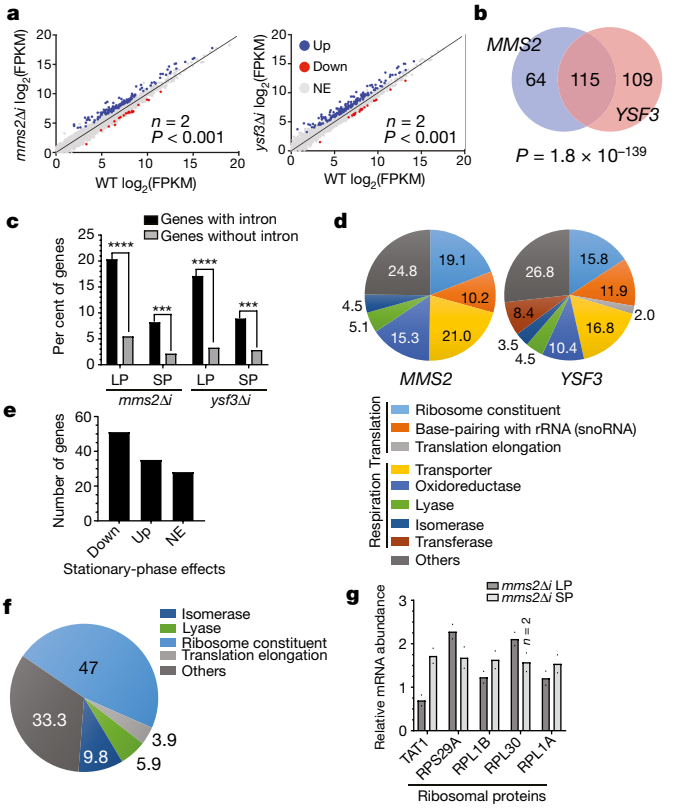

Fig. 5 | Intron deletion increases the expression of genes associated with translation and respiration. a, RNA abundance (in fragments per kilobase per million reads mapped (FPKM)) of wild-type and Δi strains (*mms2*Δ*i* and *ysf3*Δ*i*) in the stationary phase was compared using RNA sequencing. Genes that are up- or downregulated with a P value < 0.001 (t-test; one-sided) or not affected (NE) are indicated. The mean value from two biologically independent replicates is presented. **b**, Genes affected by two intron deletions were compared in the stationary phase, and the statistical significance (Fisher's exact test) of the overlap is indicated (see Methods). **c**, Per cent of genes with or without introns induced in *mms2*Δ*i* and *ysf3*Δ*i* (see Methods for sample size). χ^2 test was used to compare intron-containing genes and genes that do not contain introns. $^{***}P < 3 \times 10^{-8}$, $^{****}P < 3 \times 10^{-16}$. **d**, Gene Ontology of genes that are upregulated in stationary phase upon intron deletion. **e**, Common genes that are normally downregulated (down), upregulated (up) or not affected in stationary phase. **f**, Gene Ontology of common intron targets that are normally repressed in stationary phase. **g**, Expression levels of the five most-upregulated genes in intron deletion were determined relative to wild type in the *mms2*Δ*i* strain. Relative mRNA abundance given as $\log_2$(mRNA abundance in *mms2*Δ*i*/mRNA abundance in wild type).

two Δi strains, which indicates that introns affect gene expression independently of the function of their host gene (Extended Data Fig. 8e). Whereas only 4% of the yeast genes contain an intron, more than 15% of intron-containing genes—and only 5% of all genes without an intron—were upregulated in Δi strains (Fig. 5c). This result is consistent with the notion that intron deletion induces gene expression at least in part through the modification of splicing.

Intron deletion modified the expression of 15% of the genes that are repressed in the stationary phase (Fig. 5a and Extended Data Fig. 8a–c). Notably, 30% of the upregulated genes in Δi strains are intron-containing genes, which suggests that intron deletion particularly deregulates the repression of intron-containing genes. The effect on gene expression is not linked to specific introns and could be detected in a variety of Δi strains (Supplementary Table 5). We conclude that introns have common functions that lead to the repression of genes associated with nutrient depletion and the stationary phase.

Introns mediate the repression of RPGs

Gene Ontology analysis identified two major categories of genes that are upregulated in Δi strains and these were not identified in those that are downregulated (Fig. 5d and Extended Data Fig. 8b). One of the two categories contains translation-related genes (including RPGs) and the other includes different types of respiration-associated genes (Fig. 5d). Both categories were further enriched in genes that are normally repressed under starvation (Fig. 5e, f). Therefore, intron deletion specifically upregulates a well-defined set of genes associated with ribosome production, which are regulated at least in part by the nutrient-sensitive target of rapamycin (TOR) pathway[11]. Among the top five protein-coding genes that are repressed during starvation in an intron-dependent manner, two contain

© 2019 Springer Nature Limited. All rights reserved.

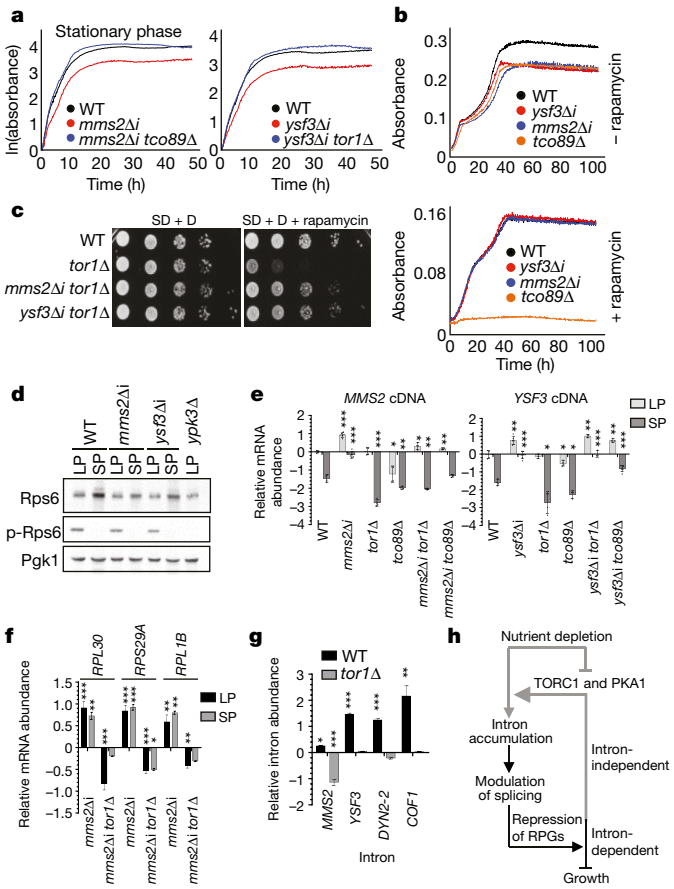

Fig. 6 | Introns promote nutrient-dependent repression of ribosome biogenesis. a, Growth profiles of wild-type cells, cells that lack introns (*mms2Δi* or *ysf3Δi*) or that lack both introns and a TORC1 gene (*mms2Δi tco89Δ* or *ysf3Δi tor1Δ*) in synthetic minimal medium (SD). **b**, Growth profiles of *mms2Δi*, *ysf3Δi*, wild-type and *tco89Δ* cells in medium with (+) or without (−) rapamycin. **c**, Growth profile of *tor1Δ*, *mms2Δi tor1Δ* and *ysf3Δi tor1Δ* strains in minimal medium with dextrose (SD + D) with (+ rapamycin) or without rapamycin. **d**, The phosphorylation of the TORC1 target Rps6 was examined in wild-type, *mms2Δi* and *ysf3Δi* strains in the log phase and stationary phase. Rps6 was detected using general or phosphorylation-specific antibodies (p-Rps6 denotes phosphorylated Rps6). The *ypk3Δ* strain was included as phosphorylation control and Pgk1 was included as a loading control. For gel source data, see Supplementary Fig. 1. Data in **a**–**d** are representative of three independent biological replicas. **e**, The abundance of *YSF3* and *MMS2* mRNAs in the presence or the absence of introns was determined in *tor1Δ* and *tco89Δ* strains in both log phase and stationary phase. Relative mRNA abundance is given as $\log_2$(mRNA abundance of the gene in each condition or strain/mRNA abundance of the gene in wild-type LP). Differences relative to wild type in log phase or stationary phase were calculated, using a two-sided *t*-test and assuming unequal variances. $*P < 0.05$, $**P < 0.01$, $***P < 0.001$. Bars represent mean ± s.d. from two or three (*mms2Δi*, *ysf3Δi* and *ysf3Δi tco89Δ*) biologically independent strains. **f**, Expression of RPGs in *mms2Δi* and *mms2Δi tor1Δ* cells was determined in log phase and stationary phase using RT–qPCR and the $\log_2$ difference between the phases was calculated (see Methods). Differences relative to wild-type log phase or stationary phase were calculated as described in **e**. **g**, Intron abundance was determined in wild type and *tor1Δ* cells using RT–qPCR as in **f**. Relative intron abundance is given as $\log_2$(intron abundance of the gene in SP/intron abundance of the gene in LP). **h**, Model for intron-dependent regulation of gene expression under starvation conditions. The intron-dependent part of the TORC1 pathway is indicated in black. Arrowheads and short horizontal lines indicate activation and inhibition, respectively.

introns, four are TORC1-dependent RPGs and one is directly implicated in amino acid transport (which is also linked to the TOR pathway)[12,13] (Fig. 5g).

Deleting factors involved in the TORC1, but not the TORC2, pathway repressed the intron-deletion growth defect (Fig. 6a and Extended Data Fig. 9). Notably, intron deletion reduced sensitivity to rapamycin, rescued the TORC1-dependent hypersensitivity to rapamycin and did not affect the phosphorylation or the expression of early targets of TORC1 (Fig. 6b–d and Extended Data Fig. 10a), which suggests that introns function downstream of TORC1. Consistently, intron deletion induced the expression of RPGs, which are downstream targets of the TORC1 pathway (Fig. 6f). Inactivating the PKA pathway[12], which cross-interacts with TORC1 and regulates ribosome biogenesis in response to glucose, also rescued the growth defect of intron deletion (Extended Data Fig. 10b, c). The intron-dependent repression of TORC1 or PKA spliced targets, such as *RPL30*, occurred through repression of splicing (Extended Data Fig. 3d, e). Deleting the TORC1 components *TOR1* and *TCO89* did not consistently alter the abundance of the spliced forms of *YSF3* and *MMS2*, but instead repressed the accumulation of introns under starvation conditions (Fig. 6e, g). This suggests that TORC1 induces the accumulation of introns when nutrients are depleted, which in turn reinforces TORC1-dependent repression of RPGs.

Discussion

We have shown that introns affect cell growth in response to nutrient depletion, regardless of host-gene function. Deleting a single intron reduces the capacity of cells to withstand nutrient depletion or starvation (Figs. 1, 2). Notably, introns could independently rescue the defects caused by intron deletion, even when their host protein was not produced (Fig. 3). Transcriptome analyses indicate that introns promote resistance to nutrient depletion by inhibiting a common set of genes that are associated with translation and respiration (Fig. 5). These intron effects appear to couple the TOR and PKA pathways to the repression of ribosome biogenesis, on the basis of nutrient concentration (Fig. 6 and Extended Data Fig. 10b, c). Together, the data present a paradigm of intron function in which the presence of introns directly contributes to cell growth in a way that is independent of the function of their host gene.

Whether introns represent a burden or an advantage for homeostasis in eukaryotic cells has been a source of debate[2,3,14]. Our results provide evidence for both sides of this hypothesis. In most cases, introns appear to be a burden on rapidly growing cells. They often reduce growth in rich medium, but provide a net advantage when nutrients are depleted (Fig. 1d). We argue from these data that, in nature, being able to control cell metabolism as a function of nutrient availability represents a major evolutionary advantage that may well compensate for the losses in growth rate in nutrient-rich environments.

Our discovery of a requirement for introns for cell survival under starvation conditions suggests a model for understanding nutrient sensing and growth regulation. This model (Fig. 6h) suggests that when nutrients are depleted, introns accumulate in a TORC1-dependent manner and this accumulation reinforces the repression of RPGs that are controlled by the TORC1 and PKA pathways. This, in turn, reduces nutrient consumption and promotes cell survival. The intron-dependent repression of RPGs is dependent on the modulation of splicing. Inhibition of spliceosome function or expression of RPGs represses the effect of intron deletion (Extended Data Fig. 3). This suggests that the accumulation of introns under starvation conditions may sequester or reduce the efficiency of the spliceosome, which enables the repression of a small group of highly expressed RPGs. This model is consistent with previous reports that show that the splicing of RPGs is selectively repressed upon nutrient depletion and that splicing efficiency is established through competition between spliced RNAs[10,15].

Online content

Any methods, additional references, Nature Research reporting summaries, source data, statements of data availability and associated accession codes are available at https://doi.org/10.1038/s41586-018-0859-7.

© 2019 Springer Nature Limited. All rights reserved.

Received: 23 February 2018; Accepted: 7 December 2018;
Published online 16 January 2019.

1. Irimia, M. & Roy, S. W. Origin of spliceosomal introns and alternative splicing. *Cold Spring Harb. Perspect. Biol.* **6**, a016071 (2014).
2. Jo, B. S. & Choi, S. S. Introns: the functional benefits of introns in genomes. *Genomics Inform.* **13**, 112–118 (2015).
3. Neuvéglise, C., Marck, C. & Gaillardin, C. The intronome of budding yeasts. *C. R. Biol.* **334**, 662–670 (2011).
4. Hooks, K. B., Delneri, D. & Griffiths-Jones, S. Intron evolution in Saccharomycetaceae. *Genome Biol. Evol.* **6**, 2543–2556 (2014).
5. Hartung, F., Blattner, F. R. & Puchta, H. Intron gain and loss in the evolution of the conserved eukaryotic recombination machinery. *Nucleic Acids Res.* **30**, 5175–5181 (2002).
6. Spingola, M., Grate, L., Haussler, D. & Ares, M. Jr. Genome-wide bioinformatic and molecular analysis of introns in *Saccharomyces cerevisiae*. *RNA* **5**, 221–234 (1999).
7. Parenteau, J. et al. Deletion of many yeast introns reveals a minority of genes that require splicing for function. *Mol. Biol. Cell* **19**, 1932–1941 (2008).
8. Cox, J. S. & Walter, P. A novel mechanism for regulating activity of a transcription factor that controls the unfolded protein response. *Cell* **87**, 391–404 (1996).
9. Gray, J. V. et al. "Sleeping beauty": quiescence in *Saccharomyces cerevisiae*. *Microbiol. Mol. Biol. Rev.* **68**, 187–206 (2004).
10. Munding, E. M., Shiue, L., Katzman, S., Donohue, J. P. & Ares, M. Jr. Competition between pre-mRNAs for the splicing machinery drives global regulation of splicing. *Mol. Cell* **51**, 338–348 (2013).
11. González, A. & Hall, M. N. Nutrient sensing and TOR signaling in yeast and mammals. *EMBO J.* **36**, 397–408 (2017).
12. Martin, D. E., Soulard, A. & Hall, M. N. TOR regulates ribosomal protein gene expression via PKA and the Forkhead transcription factor FHL1. *Cell* **119**, 969–979 (2004).
13. Peter, G. J., Düring, L. & Ahmed, A. Carbon catabolite repression regulates amino acid permeases in *Saccharomyces cerevisiae* via the TOR signaling pathway. *J. Biol. Chem.* **281**, 5546–5552 (2006).
14. de Souza, S. J., Long, M. & Gilbert, W. Introns and gene evolution. *Genes Cells* **1**, 493–505 (1996).
15. Pleiss, J. A., Whitworth, G. B., Bergkessel, M. & Guthrie, C. Rapid, transcript-specific changes in splicing in response to environmental stress. *Mol. Cell* **27**, 928–937 (2007).

Acknowledgements This work was supported by NSERC and a Research Chair in RNA Biology and Cancer Genomics (S.A.E.). We thank M. Ares Jr for discussion and for providing the yeast strains used in Extended Data Fig. 3e; R. Wellinger, B. Chabot and M. Scott for critical reading of the manuscript; and C. Nour Abou Chakra for reviewing the statistical analyses. Sequencing libraries were prepared by the Université de Sherbrooke RNomics Platform and sequenced in the Centre of Applied Genomics (Toronto).

Reviewer information *Nature* thanks S. Montgomery and the other anonymous reviewer(s) for their contribution to the peer review of this work.

Author contributions J.P. designed and performed experiments, analysed data, produced figures and participated in the writing of the paper. L.M., M.C. and V.G performed experiments, M.B. performed RNA sequencing data analysis. S.A.E. planned the work, proposed and designed experiments, analysed data and wrote the paper.

Competing interests The authors declare no competing interests.

Additional information
Extended data is available for this paper at https://doi.org/10.1038/s41586-018-0859-7.
Supplementary information is available for this paper at https://doi.org/10.1038/s41586-018-0859-7.
Reprints and permissions information is available at http://www.nature.com/reprints.
Correspondence and requests for materials should be addressed to S.A.
Publisher's note: Springer Nature remains neutral with regard to jurisdictional claims in published maps and institutional affiliations.

© 2019 Springer Nature Limited. All rights reserved.

METHODS

No statistical methods were used to predetermine sample size. The experiments were not randomized and investigators were not blinded to allocation during experiments and outcome assessment.

Strains and plasmids. Intron deletions were performed using two independent colonies of the strain JPY10I as previously described[7]. All deletions were carried out in diploid strains, validated using PCR and six independent haploid strains carrying the validated deletions were selected for further analyses (Fig. 1b and Extended Data Fig. 1a). The *YPK3*, TORC1, TORC2 and PKA (*TPK1*, *TPK2* and *TPK3*) deletion strains were obtained from the yeast knockout strains of Open Biosystems (*MAT*a *ura3Δ0 leu2Δ0 his3Δ1 met15Δ0*; record number 3165 for *ypk3Δ::KMX4*, record number 6864 for *tor1Δ::KMX4*, record number 2072 for *tco89Δ::KMX4*, record number 1365 for *bit61Δ::KMX4*, record number 7168 for *bit2Δ::KMX4*, record number 2264 for *slm1Δ::KMX4*, record number 7372 for *slm2Δ::KMX4*, record number 6201 for *avo2Δ::KMX4*, record number 1261 for *tpk1Δ::KMX4*, record number 1089 for *tpk2Δ::KMX4* and record number 5016 for *tpk3Δ::KMX4*). The strains *prp4-1*, *prp11-1* and *GAL-IFH1* were provided by M. Ares[10]. The double mutants (Δi/ΔTORC, Δi/ΔPKA, Δi/*prp4-1*, Δi/*prp11-1*, Δi/*GAL-IFH1* and *mms2Δi ysf3Δi*) were made by mating Δi strains together, or with a TORC1, TORC2 or PKA deletion strain, or with the *prp4-1*, *prp11-1* or *GAL-IFH1* strain. The resulting diploid strain was sporulated to produce cells that contained the double-mutated genes. To amplify the yeast *MMS2* gene with or without intron from wild-type or *mms2Δi* genomic DNA, we used the following primers for PCR: XhoI_MMS2_ for 5′-CTCCTCCTCGAGTTGTCCATTTGTACTGCCTACGTCG-3′ (the underlined bases are complementary to position −391 to −367 relative to the *MMS2* translational start site, and the 5′ extension contains an XhoI site) and BamHI_MMS2_rev 5′-ATTCCCGGATCCTTCTCGGCATGGGGTGAGTAAATTC-3′ (the underlined bases are complementary to position +614 to +638 relative to the *MMS2* translational start site, and the 5′ extension contains a BamHI site). To amplify the yeast *YSF3* gene from wild-type genomic DNA, we used the following primers for PCR: XhoI_YSF3_for 5′-CTCCTCCTCGAGCACCTCTTCCGTTAAAATGCTTGCC-3′ (the underlined bases are complementary to position −414 to −390 relative to the *YSF3* translational start site, and the 5′ extension contains an XhoI site) and BamHI_YSF3_rev 5′-ATTCCCGGATCCCCTGTTTATGACTTCACGCGACATG-3′ (the underlined bases are complementary to position +587 to +611 relative to the *YSF3* translational start site, and the 5′ extension contains a BamHI site). The PCR products were digested with XhoI and BamHI and cloned into pRS316 (*CEN6*, *ARSH4* plasmid)[16] to generate pMMS2, pmms2Δi and pYSF3. pMMS2-stop and pYSF3-stop were generated by point mutations (Bio-Basic Group). The branch-point mutation in pMMS2-stop (pBrPm) was created by mutating the branch-point sequence TACTAAC into TACTAGC. The promoter and 5′ UTR of *MMS2* were replaced in pMMS2-stop with the promoter and 5′ UTR of the *ACT1* gene (position −450 to −1 relative to the *ACT1* translational start site) to create pACT1p-UTR. To create pSWAP1 and pSWAP2, the nucleotides in position +12 to +48 and +56 to +96 relative to the *MMS2* translational start site were replaced with those in position +11 to +47 and +279 to +319 relative to the *ACT1* translational start site, respectively, in pMMS2-stop. pMMS2-unfolded was created by mutating the nucleotides TT in position −10 and −9 relative to the *MMS2* translational start site into CG in pMMS2-stop, and pMMS2-refolded was created by mutating the TT into GA and the nucleotides AA in position +65 and +66 relative to the *MMS2* translational start site into TC in pMMS2-stop. The plasmid pMMS2-YSF3 was made by replacing the exon 2 of *MMS2* with that of *YSF3* in pMMS2-stop. To create the *MMS2*-unfolded and -refolded strains, the 5′ UTR, exon 1 and intron of the chromosomal copy of the *MMS2* gene were replaced with the *URA3* gene using standard PCR-based gene replacement[16] and this strain was transformed with a PCR fragment containing the *MMS2*-unfolded or -refolded sequences amplified from the pMMS2-unfolded and pMMS2-refolded plasmids, respectively. Loss of the *URA3* marker was determined by growing cells on medium containing 5-fluoroorotic acid[17].

pMMS2-YSF3I was created by replacing the *MMS2* intron with that of *YSF3* in pMMS2-stop. pADH1t was made by replacing the nucleotides +500 to +638 relative to the *MMS2* translational start site with those in position +1048 to +2239 relative to the *ADH1* translational start site in pMMS2-stop. To amplify the yeast *TUB1* gene from wild-type genomic DNA, we used the following primers for PCR: SalI_TUB1_for 5′-ACGCGTCGACGCATCTAGCGATATATTCCAGAGGAAC-3′ (the underlined bases are complementary to position −423 to −397 relative to the *TUB1* translational start site, and the 5′ extension contains an SalI site) and BamHI_TUB1_rev 5′-ATTCCCGGATCCGGCCCATCAACTACGATGAGACTTAC-3′ (the underlined bases are complementary to position +1657 to +1682 relative to the *TUB1* translational start site, and the 5′ extension contains a BamHI site). The PCR products were digested with SalI and BamHI and cloned into pRS316[16] to generate pTUB1. The plasmid pMMS2-TUB1 was created by replacing the 5′ UTR, exon 1 and intron of *TUB1* with those of *MMS2* in pTUB1. The plasmids YFP-MMS2I and YFP-YSF3I were made by inserting the promoter of *RPS28A* (nucleotides −285 to −1 relative to its translational start site) upstream of the yellow fluorescent protein (YFP) fragment[18] where the *MMS2* or *YSF3* introns were embedded at position +196 relative to the YFP translational start site followed by the terminator sequence of *ADH1* in pRS315[16]. Yeast cells were transformed by a modification[19] of the lithium acetate method[20] and were grown in standard yeast medium[21,22]. All plasmids were propagated in bacteria using standard *Escherichia coli* strains and growth conditions[23].

RNA extraction, qPCR analysis and splicing index analysis. Total RNA was isolated from cells grown in log phase or stationary phase using a commercial kit (Omega Bio-Tek). DNase treatment (Qiagen) was performed and 50 ng was reverse-transcribed using Transcriptor Reverse Transcriptase (Roche). PCR was performed in a Realplex (BioRad) as previously described[24]. In general, the assays included three biological and two technical replicates. RNA levels were normalized to unrelated RNAs (for example, *Spt15*, *Act1*, *Nme1* or *Aro3*). For splicing index, end-point PCR (30 cycles) was performed using Platinum Taq (Invitrogen Life Technologies) and 10 ng of cDNA as previously described[25]. The per cent splicing index was calculated by dividing the amount of unspliced over total RNA, × 100. The primers used for real-time PCR and splicing index are listed in Supplementary Table 6.

Western blot analysis. Cell extracts were prepared from cells grown in log phase or stationary phase. Cell pellets were resuspended in lysis buffer (50 mM Tris-HCl pH 7.5, 150 mM NaCl, 15% glycerol, 0.5% Tween-20, PhosSTOP phosphatase inhibitors (Roche) and cOmplete Mini EDTA-free protease inhibitors (Roche)) as previously described[26]. Lysis was performed with glass beads by shaking in a Precellys 24 tissue homogenizer (Bertin Corp.) at 5,000 rpm for 5 cycles of 30 s with 30 s on ice between the cycles. Debris was removed from the lysate by centrifugation at 13,000 rpm for 15 min at 4 °C. Proteins (10 μg for log-phase samples and 20 μg for stationary-phase samples) were separated on 10% SDS–PAGE and transferred to Protran nitrocellulose membranes (GE Healthcare). Membranes were blocked with 5% BSA in TBS-T (20 mM Tris-HCl pH 7.6, 150 mM NaCl, 0.1% Tween-20) for 90 min at room temperature and incubated overnight at 4 °C with primary antibodies diluted in TBS-T with 5% BSA (1:1,000 for rabbit anti-RPS6 (#ab40820, Abcam), 1:1,000 for rabbit anti-phospho-Ser235/Ser236-S6 (#2211, Cell Signaling Technology) and 1:10,000 for mouse anti-PGK1 (#459250, Invitrogen). Membranes were incubated for 90 min at room temperature with horseradish peroxidase (HRP)-conjugated secondary antibodies diluted in TBS-T with 5% BSA (1:5,000 for donkey anti-rabbit IgG (#NA934V, GE Healthcare), 1:2,000 for sheep anti-mouse IgG (#NA931V, GE Healthcare). Revelation was done using Western Lightning Plus-ECL reagents (Perkin Elmer) and data were acquired on a LAS4000 system (GE Healthcare).

Growth assays. For growth assays in low-phosphate (5%) or low-glucose (0.1%) medium, 3.36×10^7 cells in log phase were collected by centrifugation and resuspended in 1 ml of synthetic minimal medium (SD) containing 1.7 g/l of yeast nitrogen base without amino acids and ammonium sulfate (BioShop), 1 g/l of L-glutamic acid (Aldrich) supplemented with the appropriate amino acids to permit cell growth, and 2% of D-glucose (BioShop). Five microlitres of yeast cells suspension was added to 95 μl of SD plus appropriate amino acids and 2% D-glucose (SD + D) or glucose-depletion medium (SD − D) or in phosphate-deprivation medium (SD − P) plus 2% D-glucose in a 96-well plate. SD − P medium was prepared as previously described[27]. Growth curve analysis was performed as described[7,28]. The growth assays were performed with at least three biological and two technical replicates. The growth assays were usually performed at 30 °C except for the *prp4-1*, *prp11-1* and *GAL-IFH1* mutants, which were performed at 25 °C.

Starvation and re-growth assays. The yeast strains were grown overnight in 100 μl of SD + D supplemented with histidine, leucine, uracil and lysine in a 96-well plate. The cells were diluted to 2.5×10^6 cells/ml in 100 μl of SD with histine, leucine, uracil, lysine and 2% of D-glucose in a 96-well plate and incubated 7 h at 30 °C with shaking. Equal quantities of wild type and 94 Δi strains (2.5×10^6 cells) were mixed together and 1.67×10^4 cells/ml of the mixed culture were inoculated in 400 ml of SD with histine, leucine, uracil, lysine and 2% of D-glucose in a bioreactor (Infors-HT) in triplicate. Cultures were incubated for 200 h to allow the cells to reach late stationary phase. Then the cells were diluted to 3.33×10^6 cells/ml in 400 ml of new medium and re-grown for 10–12 h. Total genomic DNA of 1×10^8 cells was isolated at the beginning of the culture when all 94 Δi and wild-type strains in a given mix were detected, and at different time points as the culture grew. DNA extraction was performed using glass beads, as described[29,30]. The ratio of each strain was calculated by end-point PCR using boundary-spanning primers (BSP) and compared to the previous time point. End-point PCR (30 cycles) was performed using Platinum Taq (Invitrogen Life Technologies) on 5 ng of total genomic DNA as previously described[25]. Amplicon amount of each Δi strain in pre-stationary phase, stationary phase and log phase of the re-growth assay was divided by the amplicon amount at time 0. This ratio was divided by the average ratio of two amplicons found in all strains (wild type or Δi strains *RPL8B* and *SPT15*). The relative starvation ratio was the ratio in stationary phase divided by the ratio in pre-stationary phase; and the relative re-growth ratio was the ratio in log phase of the re-growth assay divided by the ratio in stationary phase.

© 2019 Springer Nature Limited. All rights reserved.

Nutrient-depletion assay. The first steps were identical to the starvation assay, except that 1.67×10^6 cells/ml of the mixed culture were inoculated in triplicate in 25 ml of SD − P plus 2% D -glucose or SD − D and incubated at 30 °C for 24 or 70 h, respectively. The mixed cultures were diluted each day (to 1.67×10^6 cells/ml) in SD low-phosphate (2% phosphate) or in SD low D-glucose (0.2% D-glucose) until 152 doublings (±2) were reached. The number of culture duplication was calculated using this equation: $G = \ln(C_f/C_i)/\ln(2)$, in which G represents the number of duplications, and C_f and C_i are the final and the initial concentration of cells of the mixed cultures, respectively. Total genomic DNA of 1×10^8 cells was isolated at different time points and the ratio of each strain was calculated by end-point PCR using BSP and compared to time 0, as described in the starvation and re-growth assays.

Data analyses. Overall, standard analysis methods that are routinely reported in the literature were used. As all experiments such as intron deletions and other tested conditions were conducted separately, all events and measurements were considered independently. Generally, the average value is shown, and in bar graphs the standard deviations are indicated by error bars. Unless otherwise indicated, two-sided statistical tests and a $P < 0.05$ significance level were used. Differences between RT–qPCR groups or wild type versus Δi were calculated using a two-sided *t*-test assuming unequal variances. The prop.test in R (version 3.3.0) was used to compare positive and negative effects, or to compare genes with introns versus genes without introns using χ^2 test. For Fig. 5c, the sample size (n) is 402 genes for log phase and 158 genes for stationary phase in *mms2*Δ*i*, and 255 genes for log phase and 204 genes for stationary phase in *ysf3*Δ*i*, and the number of genes with and without an intron is 280 and 6,282 genes, respectively. For Fig. 6f, g, each bar represents the $\log_2$ of the difference between phases of three biologically independent mutant strains and two biologically independent wild-type strains ($\log_2(\text{difference}) = \log_2(\text{mean}_{\text{mutant}})/(\text{mean}_{\text{WT}})$). The error bars (s.d.) were calculated with this equation:

$$\text{s.d.} = \log_2(\text{difference}) \times \sqrt{(\text{s.d.}_{\text{mutant}}/\text{mean}_{\text{mutant}})^2 + (\text{s.d.}_{\text{WT}}/\text{mean}_{\text{WT}})^2 - 2 \times ((\text{s.d.}_{\text{mutant}} \times \text{s.d.}_{\text{WT}})(\text{mean}_{\text{mutant}} \times \text{mean}_{\text{WT}}))}$$

Spot test assay. The yeast strains were grown overnight in 3 ml SD + D. Five ten-fold dilutions were made in a 96-well plate in 200 µl of total water, to obtain 2×10^6 to 200 cells per ml. Five microlitres of each dilution were spotted on SD + D with or without 1ng/ml of rapamycin. The plates were incubated for 2 to 3 days at 30 °C.

Preparation of RNA samples and RNA sequencing. Ribosomal RNAs were depleted from 5 µg of DNase treated-RNA, using Ribo-Zero rRNA removal kit from Illumina. The RNA sequencing library was built as previously described[31] by the RNomics Platform of the Université de Sherbrooke (http://rnomics.med.usherbrooke.ca). Wild-type and Δi libraries were multiplexed, and sequencing was done in biological duplicate. Pooled libraries were sequenced at 126-bp paired-end reads and a read depth that varied between 36 and 60 million reads was obtained using Illumina HiSeq 2500 at The Centre for Applied Genomics (Toronto). All samples were subjected to saturation tests and coverage, and coverage was found adequate in all cases. Sequence reads were aligned on a transcriptome reference sequence database (sacCer3) using the Bowtie v.2 aligner (default parameters) and all valid mapping positions were kept. Genes were quantified in FPKM using Cufflinks v.2[32]. Introns were quantified using correct count analysis pipeline (CoCo) (http://gitlabscottgroup.med.usherbrooke.ca/scott-group/coco)[33]. Fold changes (expressed in base 2 logarithm) were then calculated between each group of samples using the DESeq2 Bioconductor R package[34], and results with a P value < 0.001 (*t*-test one-sided) were considered significant. The significance of the variation in sequence was assessed using a P value adjustment method that uses the Benjamini–Hochberg method for multiple testing[35]. DESeq2 provides methods to test for differential expression by use of negative binomial generalized linear models; the estimates of dispersion and logarithmic fold changes incorporate data-driven prior distributions[36].

Secondary structure prediction. Introns that accumulate when nutrients are depleted and repress growth when deleted were identified, and the structure of those with a single intron and a 5′ UTR–exon1–intron sequence shorter than 1,400 nucleotides (the average limit of the prediction tools) was predicted using two different prediction tools. The ten introns with the greatest effect on starvation are shown in Extended Data Fig. 7a. As a control, we also predicted the structure of five introns that do not accumulate during starvation or affect growth when deleted, and present one example in Extended Data Fig. 7b. The 5′ UTR boundaries were obtained from transcriptome sequencing[37]. The structures were predicted essentially as previously described, with few modifications[38]. Each structure was predicted using the default setting[39] of mfold and CLC Main Workbench secondary-structure-analysis tool, Build 1305231204. Minima of 14 suboptimal structures were sampled and only structures with a d_G of −11.34 or smaller, and which were reproduced by both folding tools, were used. To identify mutations that disrupt or restore intron structure, nucleotide substitutions were introduced, the structure calculated as described above, and then mutations with the anticipated structural effects were tested in vivo.

Gene Ontology analysis. The Gene Ontology (GO) analyses were conducted using the SGD server (https://www.yeastgenome.org/). The statistical significance associated with a particular GO term within a group of genes in the list was determined using the default settings of GO Term Finder: a P value < 0.01 represents the probability of observing at least x number of genes out of the total (n) genes in the list annotated to a particular GO term, given the proportion of genes in the whole genome that are annotated to that GO Term. The GO terms shared by the genes in the list are compared to the background distribution of annotation. The false discovery rate was calculated for each node by running 50 simulations with random genes, and counting the average number of times a P value as good as or better than a P value generated from the real data was seen. To assess $P = 1.8 \times 10^{-139}$, Fisher's exact test was performed based on the 6,796 genes expressed in our RNA sequencing data as described[40].

Reporting summary. Further information on research design is available in the Nature Research Reporting Summary linked to this article.

Data availability

Supplementary Data are available online. Additional data generated in this study have been submitted to the NCBI Gene Expression Omnibus (GEO; https://www.ncbi.nlm.nih.gov/geo) under the accession number GSE111056. All strains are available upon request.

16. Sikorski, R. S. & Hieter, P. A system of shuttle vectors and yeast host strains designed for efficient manipulation of DNA in *Saccharomyces cerevisiae*. *Genetics* **122**, 19–27 (1989).
17. Boeke, J. D., Trueheart, J., Natsoulis, G. & Fink, G. R. 5-Fluoroorotic acid as a selective agent in yeast molecular genetics. *Methods Enzymol.* **154**, 164–175 (1987).
18. Yofe, I. et al. Accurate, model-based tuning of synthetic gene expression using introns in *S. cerevisiae*. *PLoS Genet.* **10**, e1004407 (2014).
19. Gietz, R. D. & Woods, R. A. Transformation of yeast by lithium acetate/single-stranded carrier DNA/polyethylene glycol method. *Methods Enzymol.* **350**, 87–96 (2002).
20. Ito, H., Fukuda, Y., Murata, K. & Kimura, A. Transformation of intact yeast cells treated with alkali cations. *J. Bacteriol.* **153**, 163–168 (1983).
21. Zakian, V. A. & Scott, J. F. Construction, replication, and chromatin structure of TRP1 RI circle, a multiple-copy synthetic plasmid derived from *Saccharomyces cerevisiae* chromosomal DNA. *Mol. Cell. Biol.* **2**, 221–232 (1982).
22. Rose, M. D., Winston, F. & Hieter, P. *Methods in Yeast Genetics: A Laboratory Course Manual* (Cold Spring Harbor Laboratory, Cold Spring Harbor, 1990).
23. Sambrook, J., Fritsch, E. F. & Maniatis, T. *Molecular Cloning: A Laboratory Manual*, 2nd edition (Cold Spring Harbor Laboratory, Cold Spring Harbor, 1989).
24. Brosseau, J. P. et al. High-throughput quantification of splicing isoforms. *RNA* **16**, 442–449 (2010).
25. Klinck, R. et al. Multiple alternative splicing markers for ovarian cancer. *Cancer Res.* **68**, 657–663 (2008).
26. González, A. et al. TORC1 promotes phosphorylation of ribosomal protein S6 via the AGC kinase Ypk3 in *Saccharomyces cerevisiae*. *PLoS ONE* **10**, e0120250 (2015).
27. Rubin, G. M. Preparation of RNA and ribosomes from yeast. *Methods Cell Biol.* **12**, 45–64 (1975).
28. Toussaint, M. et al. A high-throughput method to measure the sensitivity of yeast cells to genotoxic agents in liquid cultures. *Mut. Res.* **606**, 92–105 (2006).
29. Huberman, J. A., Spotila, L. D., Nawotka, K. A., el-Assouli, S. M. & Davis, L. R. The in vivo replication origin of the yeast 2µm plasmid. *Cell* **51**, 473–481 (1987).
30. Wellinger, R. J., Wolf, A. J. & Zakian, V. A. *Saccharomyces* telomeres acquire single-strand TG1-3 tails late in S phase. *Cell* **72**, 51–60 (1993).
31. Boudreault, S. et al. Global profiling of the cellular alternative RNA splicing landscape during virus–host interactions. *PLoS ONE* **11**, e0161914 (2016).
32. Trapnell, C. et al. Differential analysis of gene regulation at transcript resolution with RNA-seq. *Nat. Biotechnol.* **31**, 46–53 (2013).
33. Deschamps-Francoeur, G., Boivin, V., Abou Elela, S. & Scott, M. S. CoCo: RNA-seq read assignment correction for nested genes and multimapped reads. Preprint at https://www.biorxiv.org/content/early/2018/11/29/477869 (2018).
34. Love, M. I., Huber, W. & Anders, S. Moderated estimation of fold change and dispersion for RNA-seq data with DESeq2. *Genome Biol.* **15**, 550 (2014).
35. Ferreira, J. A. The Benjamini–Hochberg method in the case of discrete test statistics. *Int. J. Biostat.* **3**, 11 (2007).
36. Liu, Y. et al. XBSeq2: a fast and accurate quantification of differential expression and differential polyadenylation. *BMC Bioinformatics* **18**, 384 (2017).
37. Nagalakshmi, U. et al. The transcriptional landscape of the yeast genome defined by RNA sequencing. *Science* **320**, 1344–1349 (2008).
38. Chaowanathikhom, M., Nuchnoi, P. & Palasuwan, D. Significance of 3′ UTR and pathogenic haplotype in glucose-6-phosphate deficiency. *Lab. Med.* **48**, 73–88 (2017).
39. Zuker, M. Mfold web server for nucleic acid folding and hybridization prediction. *Nucleic Acids Res.* **31**, 3406–3415 (2003).
40. Agresti, A. A survey of exact inference for contingency tables. *Stat. Sci.* **7**, 131–153 (1992).

© 2019 Springer Nature Limited. All rights reserved.

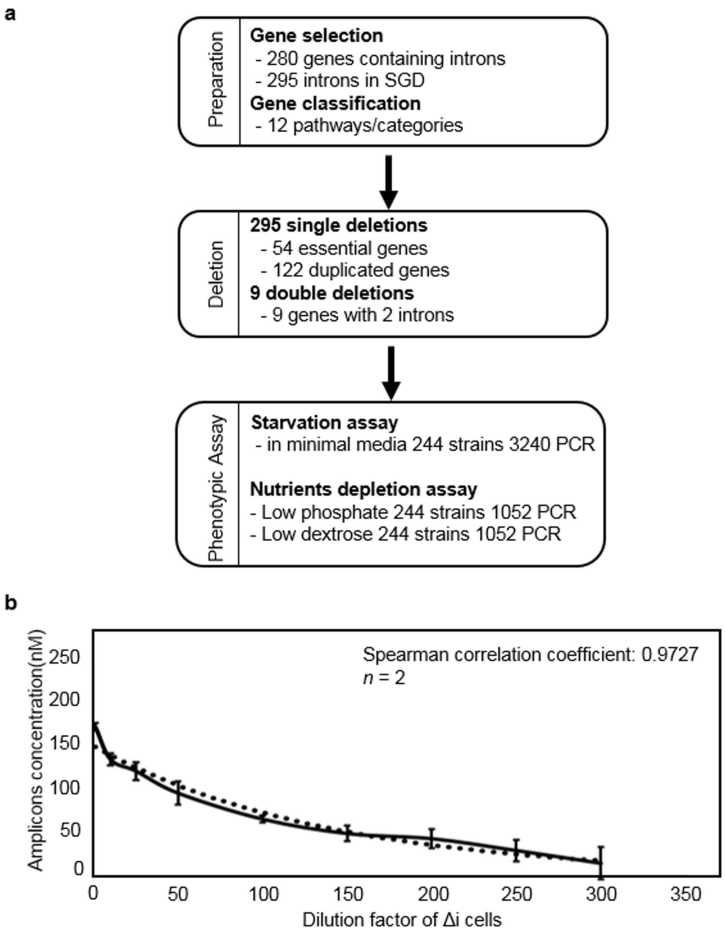

Extended Data Fig. 1 | Strategy for examining the effect of introns on cell growth and starvation. a, Summary of the pipeline used for the identification of intron functions. **b**, Validation of the BSP PCR assay to detect variation in cell number. Intron-deletion cells were diluted with wild-type cells and the BSP PCR was performed on each dilution; the amplicon amount was plotted as function of dilution. The mean value of two independent experiments is presented and the s.d. is indicated by error bars. The correlation value (Spearman correlation coefficient) is indicated. This figure is related to Fig. 1.

© 2019 Springer Nature Limited. All rights reserved.

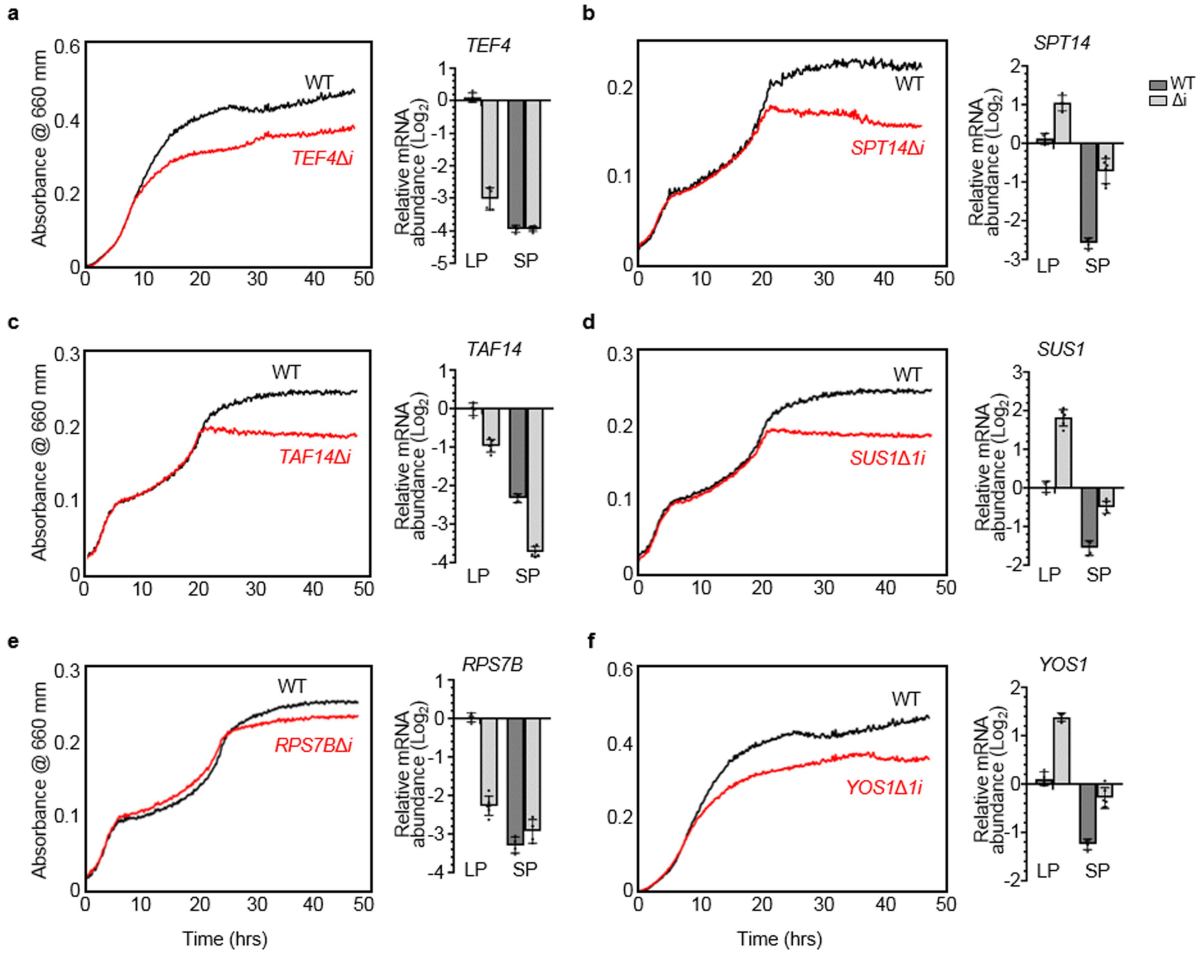

Extended Data Fig. 2 | Intron deletions inhibit cell maintenance during starvation independently of the expression pattern and function of their host gene. a–f, The growth curves of wild-type cells and Δi strains of genes with unrelated functions were determined in minimal medium with dextrose (**a**, **f**) or in minimal medium with low dextrose (**b**–**e**). The experiments were repeated independently three times with similar results. The expression profile of each host gene was determined by RT–qPCR in wild-type (dark grey) and Δi (light grey) cells in log phase or stationary phase of growth, and is presented in the form of a bar graph. The gene name is indicated in each panel. The mean value of three (two for wild type) biologically independent strains is presented and the s.d. is indicated by error bars. This figure is related to Figs. 2, 3.

© 2019 Springer Nature Limited. All rights reserved.

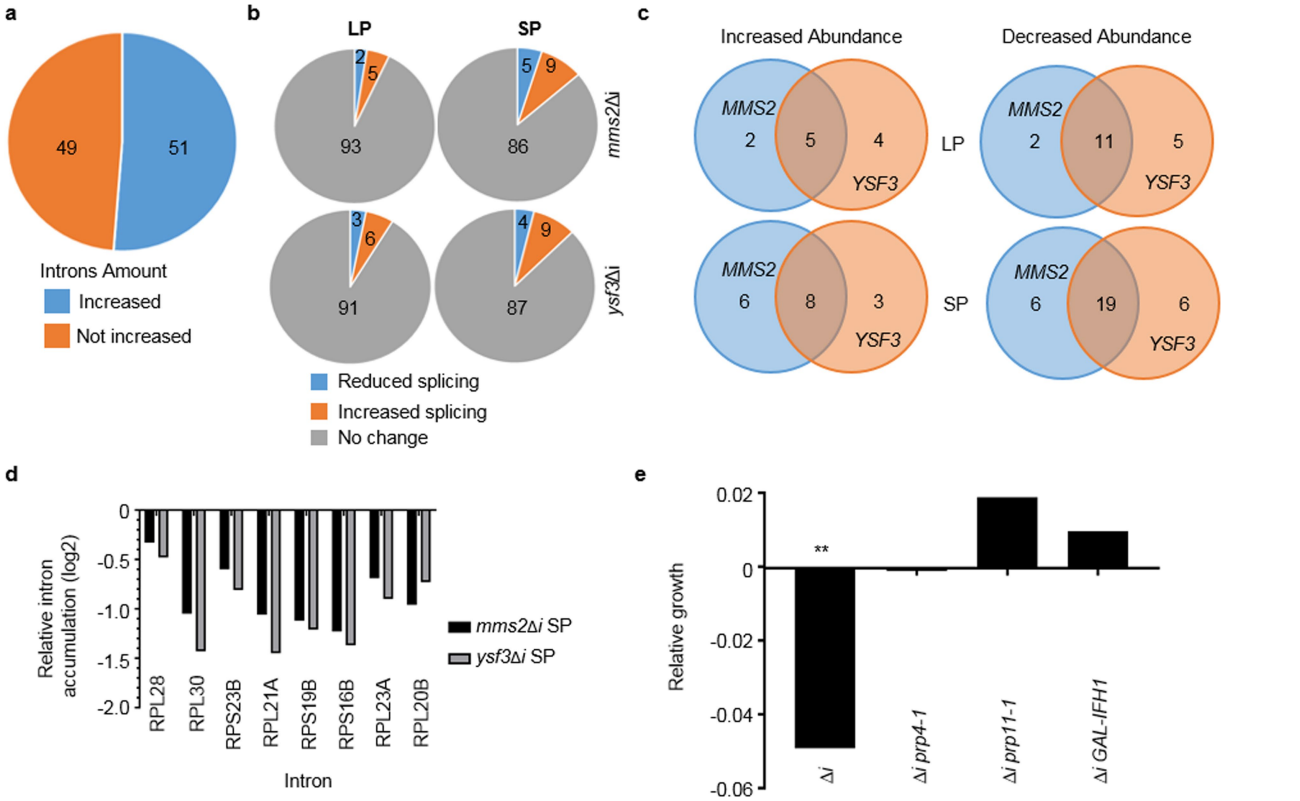

Extended Data Fig. 3 | Introns affect growth during starvation through modification of splicing. a, Introns that accumulate in the stationary phase (increased), and those that did not increase or decrease (not increased), are indicated. Intron abundance was considered to be increased when the transcripts per million (TPM) of introns at 48 h increased by more than 1.5× the TPM detected in log phase. **b**, The ratio of spliced and unspliced mRNA was calculated in cells that lack the *MMS2* or *YSF3* intron, in the log phase and stationary phase of growth; the per cent of introns is shown. **c**, The number of introns that accumulate or decrease upon the deletion of either *MMS2* or *YSF3* introns (or with both deletions) is indicated, for the log phase and stationary phase of growth. The pie charts shown are a descriptive representation of the data obtained by RNA sequencing, and the data that were validated using RT–qPCR (for example, see Fig. 3c and Supplementary Table 7). **d**, Intron deletion increases the splicing of RPGs. The intron accumulation of eight RPGs that display enhanced splicing upon the deletion of *MMS2* or *YSF3* introns is shown. Relative intron accumulation was determined between Δi and wild-type strains in stationary phase of growth as described in **b**. **e**, *MMS2* introns were deleted in wild-type cells, and in cells that express temperature-sensitive alleles of the splicing factors *PRP4* or *PRP11* or express the RPG transcription factor *IFH1* from an inducible promoter; these cells were tested for growth in low-dextrose medium at the semi-permissive temperature. The relative growth was calculated by subtracting the optical density at 660 nm ($OD_{660\,nm}$) after 96 h of growth of the Δi or double-mutant strains from that of the wild-type or the single-mutant strains, respectively. The growth assays were repeated independently three times with similar results. Differences between groups were calculated using a two-sided *t*-test assuming unequal variances. $^{**}P = 0.0044$. This figure is related to Figs. 3, 4.

© 2019 Springer Nature Limited. All rights reserved.

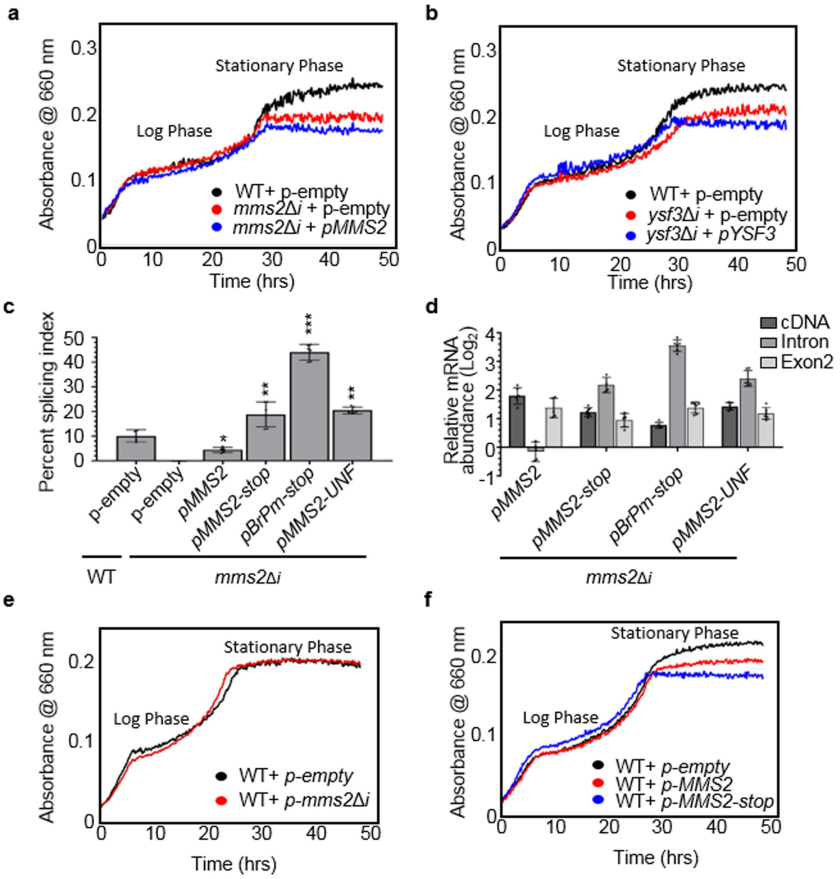

Extended Data Fig. 4 | The accumulation of the unspliced RNA and not the mature mRNA is required for cell maintenance under starvation conditions. Growth profiles of Δi cells that carry different plasmids or mutations. **a**, **b**, Expression of the host gene is not required for growth under starvation conditions. Cells that lack introns were transformed with plasmids that express the host gene of the respective intron (*mms2Δi* + pMMS2 or *ysf3Δi* + pYSF3) and the growth profile was compared to wild-type (WT + p-empty) or Δi strains (*mms2Δi* + p-empty or *ysf3Δi* + p-empty) containing empty plasmids. The experiments were repeated independently nine times with similar results. **c**, **d**, Stop-codon and branch-point mutations increase intron abundance. The splicing index (calculated by dividing the amount of unspliced over total RNA, ×100) was detected using end-point PCR, and the relative abundance of cDNA (dark grey), intronic RNA (grey) and exonic RNA (light grey) was determined using RT–qPCR. The average value of three (two for wild type) biologically independent replicates is presented and the s.d. is indicated by error bars; for **c**, differences between wild type and *mms2Δi* were calculated using two-sided *t*-test. $^{*}P = 0.013$, $^{**}P < 0.0072$, $^{***}P = 9.8 \times 10^{-8}$. **e**, **f**, Increasing the number of introns and not the host cDNA inhibits cell maintenance under starvation conditions. Growth profiles of wild-type cells transformed with empty plasmids (p-empty), plasmids expressing *MMS2* RNA (p-MMS2), *MMS2* RNA carrying a stop codon (p-MMS2-stop) and plasmid expressing *MMS2* cDNA (p-mms2Δi). The experiments were repeated independently four times with similar results. The position of the log phase and stationary phase of the growth are indicated on the growth curves. This figure is related to Fig. 3.

© 2019 Springer Nature Limited. All rights reserved.

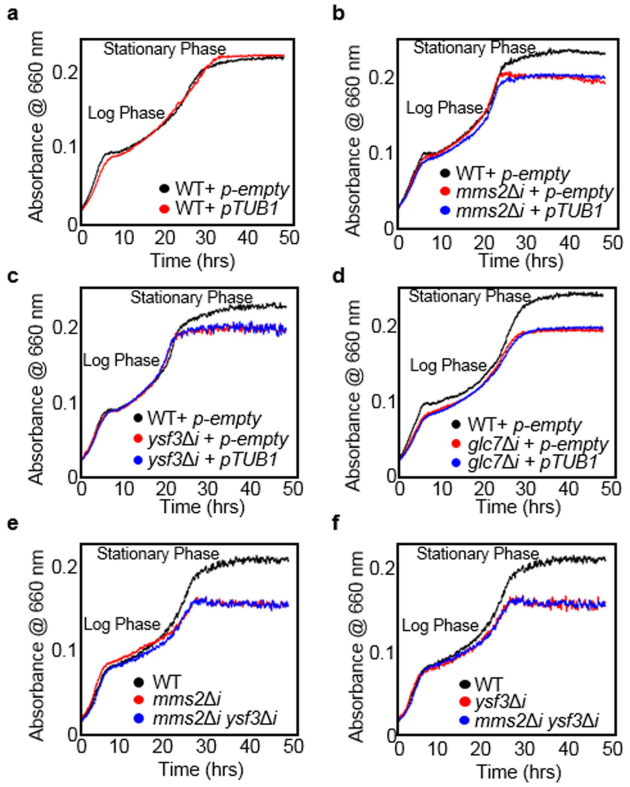

Extended Data Fig. 5 | Effect of different introns and intronic mutations on the growth of wild-type and Δi cells. a, Increasing the number of genes that contain nutrient-independent introns does not affect growth. Growth profile of wild-type cells transformed with empty plasmids or a plasmid expressing the *TUB1* gene (which contains an intron that has no effect on cell growth under starvation conditions). The experiments were repeated independently four times with similar results. **b**–**d**, Genes that contain nutrient-independent introns do not rescue the intron-deletion phenotype. Growth profile of *mms2Δi*, *ysf3Δi* or *glc7Δi* cells transformed with plasmid expressing the intron-containing *TUB1* gene. For **b**–**d**, the growth assays were repeated independently six times with similar results. **e**, **f**, Intron deletions are genetically epistatic. The growth profiles of wild-type (black), single (red) and double (blue) Δi strains were monitored for 48 h in minimal medium that is low in dextrose. The experiments were repeated independently eight times with similar results. The position of the log phase and stationary phase of the growth are indicated on the growth curves. This figure is related to Figs. 3, 4.

© 2019 Springer Nature Limited. All rights reserved.

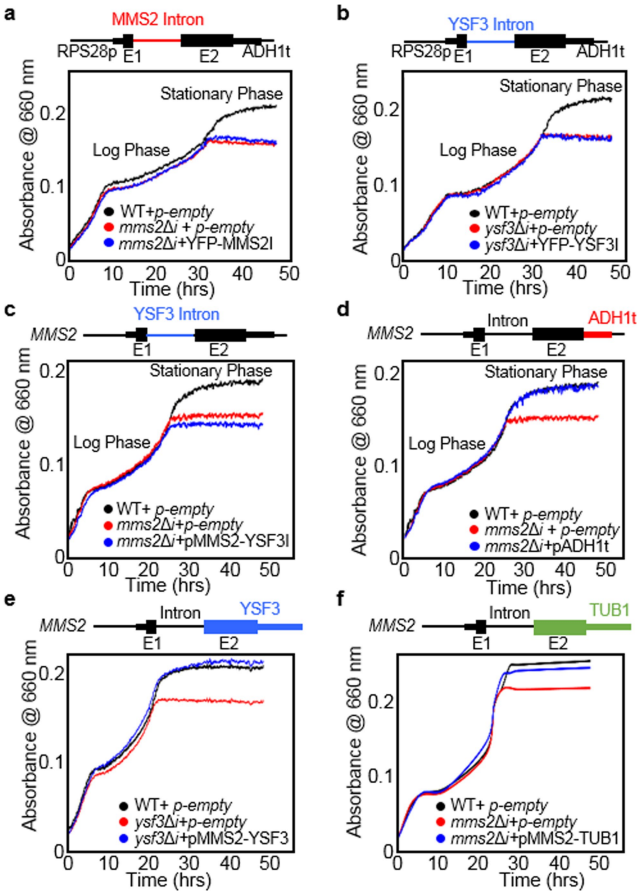

Extended Data Fig. 6 | Introns are required for cell maintenance under starvation conditions in the context of the host gene. a, **b**, Growth profile of *mms2Δi* and *ysf3Δi* cells expressing *MMS2* or *YSF3* introns from a heterologous gene (YFP-MMS2I and YFP-YSF3I). **c**, Growth profile of *mms2Δi* cells transformed with plasmid expressing a version of *MMS2* carrying the *YSF3* intron. **d**, Growth profile of *mms2Δi* cells transformed with plasmid expressing a version of the *MMS2* gene terminating with a heterologous 3′ UTR and transcription termination sequence (*ADH1t*). **e**, Growth profile of *ysf3Δi* cells transformed with plasmid expressing a version of *MMS2* carrying the exon 2 of *YSF3*. **f**, Growth profile of *mms2Δi* cells transformed with plasmid expressing a version of *MMS2* carrying the exon 2 of *TUB1*. For **a**–**f**, the experiments were repeated independently six times with similar results. The position of the log phase and stationary phase of the growth are indicated on the growth curves. This figure is related to Figs. 3, 4.

© 2019 Springer Nature Limited. All rights reserved.

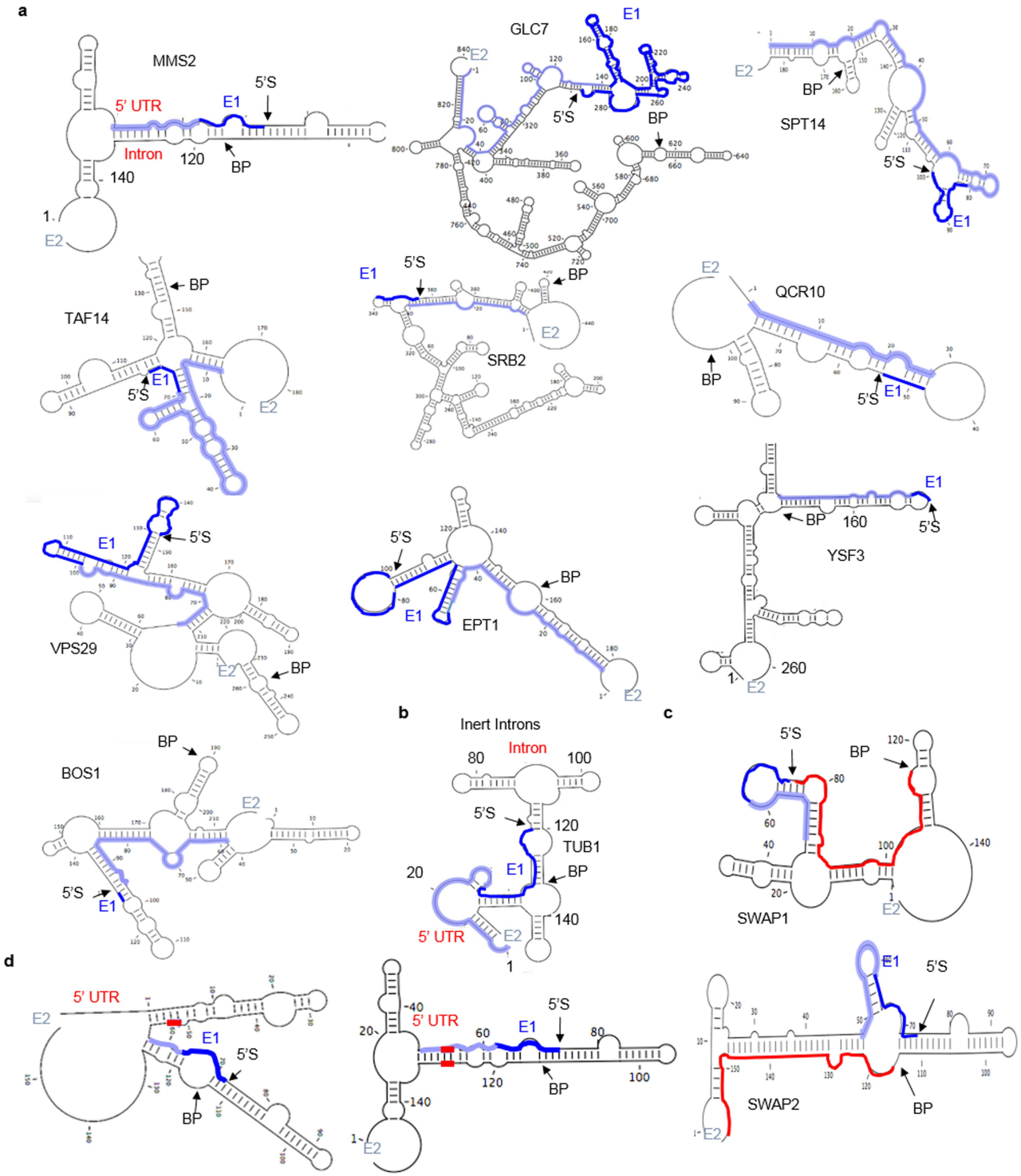

Extended Data Fig. 7 | Predicted structure of introns with different effects on growth under starvation conditions. a, The structure of the 5′ UTR, exon 1 and the intron that affects growth under starvation conditions was calculated using the mfold default setting, and the average of 15 suboptimal structures is presented. **b**, Structure of the 5′ UTR, exon 1 and the intron of the *TUB1* gene, which does not affect growth under starvation conditions. **c**, Structures of the mutated constructs tested in Fig. 4c. The substitution of the first half (SWAP1) or the second half (SWAP2) of the intron with sequence of *ACT1* intron is indicated in red. **d**, Structure of the mutated constructs tested in Fig. 4e, f. The position of the mutations that disrupt (left) or restore (right) the structure is shown in red. 5′S indicates the position of the 5′ splice site. The 5′ UTR and exon 1 are indicated in pale and dark blue, respectively. This figure is related to Fig. 4.

© 2019 Springer Nature Limited. All rights reserved.

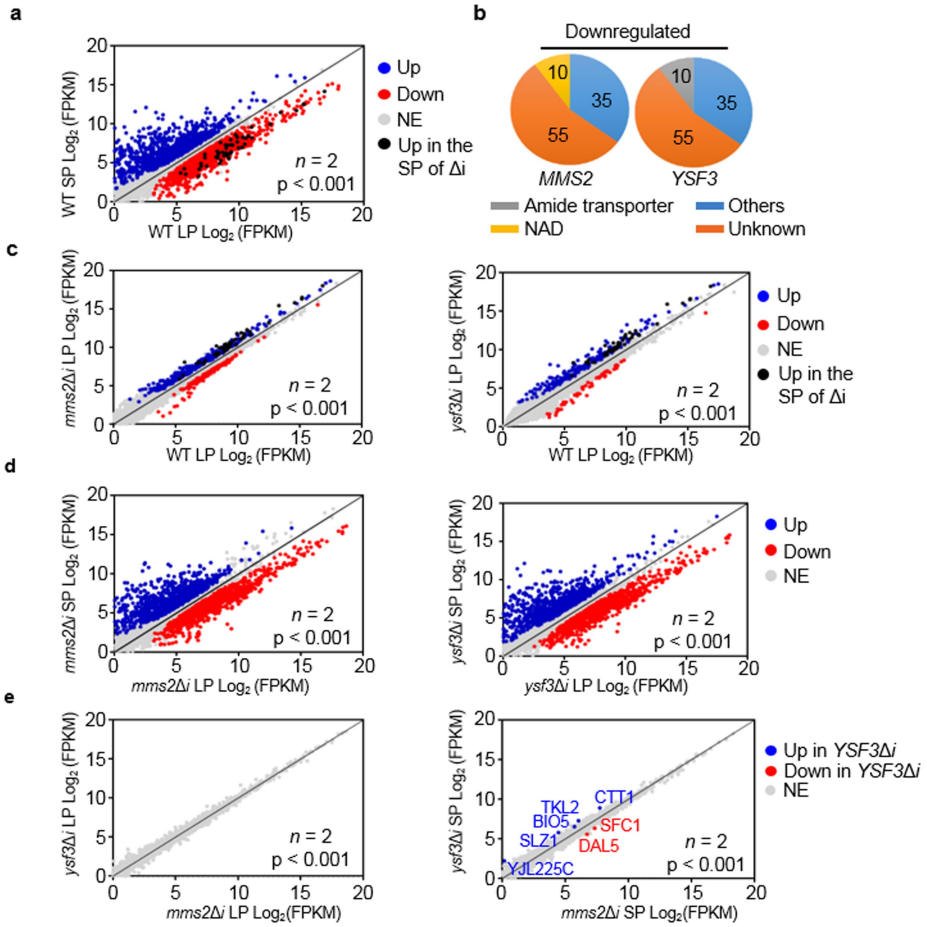

Extended Data Fig. 8 | Effect of starvation and intron deletion on gene expression. a, Comparison between the expression profiles of wild-type cells in log (WT LP) and stationary (WT SP) phases of growth. **b**, GO analysis of genes that are downregulated after the deletion of introns from *MMS2* and *YSF3* in the stationary phase of growth. The per cent of genes in each process or activity is indicated in form of a pie chart. **c**, Comparison between the expression profiles of wild-type and Δi strains in the log phase. **d**, Comparison between the expression profiles of Δi strains in log phase and stationary phase. **e**, Comparison between the expression profiles of the two Δi strains in the log phase (left) and stationary phase (right) of growth. Blue, red, grey and black dots indicate the number of genes that are upregulated, downregulated, not affected and upregulated, respectively, in Δi strains in the stationary phase. For **a**, **c**–**e**, the mean value from two biologically independent replicates is presented and the *P* value (*t*-test; one-sided) of the difference between the different strains and comparison was calculated as described in Methods, and is shown on each graph. This figure is related to Fig. 5.

© 2019 Springer Nature Limited. All rights reserved.

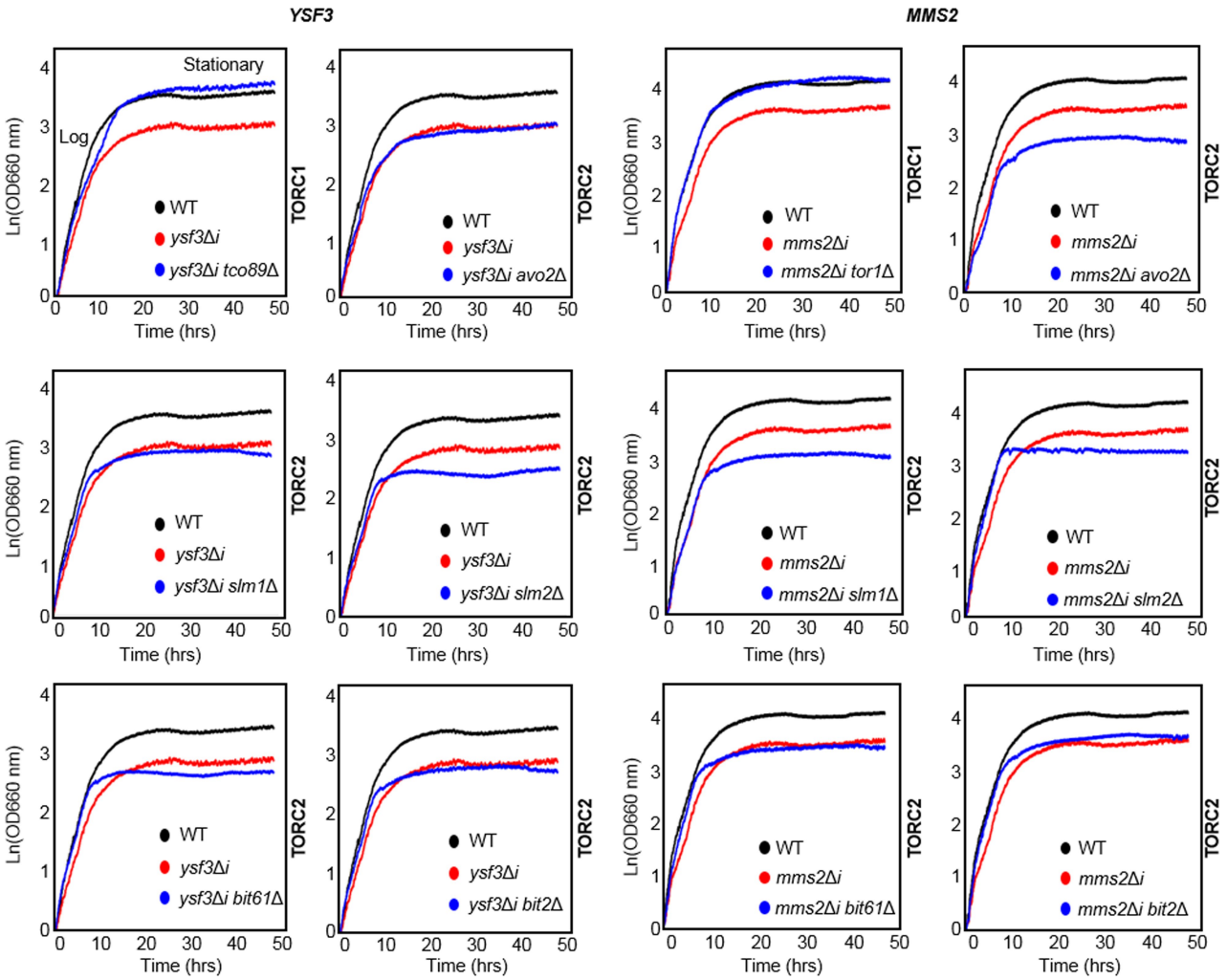

Extended Data Fig. 9 | Introns promote cell growth in a TORC1-dependent, and not TORC2-dependent, manner. The growth profile of wild-type cells, cells that lack introns or cells that lack both introns and either a component of the TORC1 (*tco89*Δ or *tor1*Δ) or TORC2 (*avo2*Δ, *slm1*Δ, *slm2*Δ, *bit61*Δ or *bit2*Δ) pathways was examined as function of the optical density of the culture in minimal medium with low dextrose. Deletions of the *YSF3* intron are shown on the left and those of *MMS2* intron are shown on the right. All these experiments were repeated independently three times with similar results. This figure is related to Fig. 6.

© 2019 Springer Nature Limited. All rights reserved.

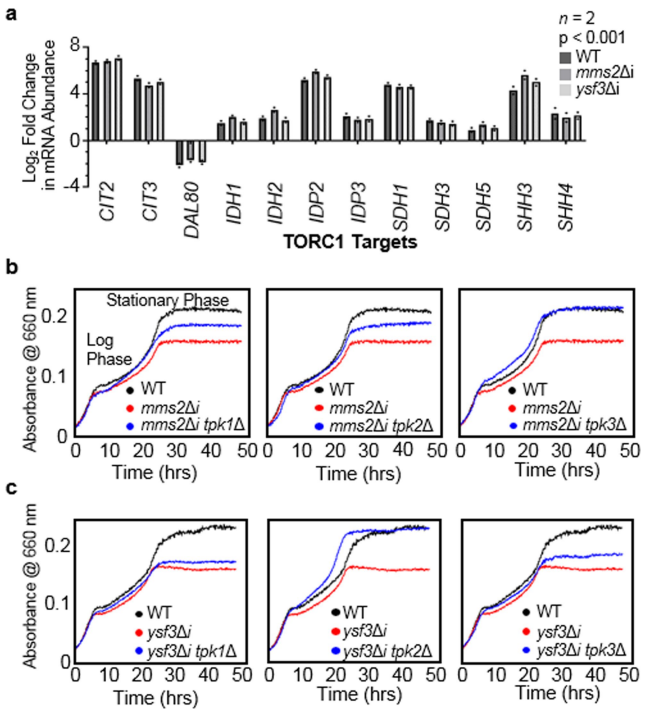

Extended Data Fig. 10 | Effect of intron deletion on the PKA pathway and the expression of TORC1 targets. a, Intron deletions do not alter the expression of TORC1 targets under starvation conditions. The expression profile of 12 regulatory targets of TORC1. The fold change (expressed as $\log_2$(mRNA abundance in SP/mRNA abundance in LP)) in RNA abundance of genes regulated by TORC1 pathway, in the log phase and stationary phase of growth, was determined using RNA sequencing in wild-type cells and cells that lack *MMS2* (*mms2Δi*) or *YSF3* (*ysf3Δi*) introns. The mean value and s.d. from two biologically independent replicates are presented. Genes are up- or downregulated with a *P* value < 0.001 (*t*-test; one-sided). **b**, **c**, Introns promote cell growth in a PKA-dependent manner. Growth profile of cells that lack different components of the PKA regulatory pathway (*TPK1*, *TPK2* and *TPK3*) in the presence or the absence of *MMS2* and *YSF3* introns. In **b**, **c**, experiments were repeated independently three times with similar results. This figure is related to Fig. 6.

© 2019 Springer Nature Limited. All rights reserved.

nature research

Corresponding author(s): Sherif Abou Elela

Reporting Summary

Nature Research wishes to improve the reproducibility of the work that we publish. This form provides structure for consistency and transparency in reporting. For further information on Nature Research policies, see Authors & Referees and the Editorial Policy Checklist.

Statistical parameters

When statistical analyses are reported, confirm that the following items are present in the relevant location (e.g. figure legend, table legend, main text, or Methods section).

n/a	Confirmed	
☐	☒	The exact sample size (*n*) for each experimental group/condition, given as a discrete number and unit of measurement
☐	☒	An indication of whether measurements were taken from distinct samples or whether the same sample was measured repeatedly
☐	☒	The statistical test(s) used AND whether they are one- or two-sided *Only common tests should be described solely by name; describe more complex techniques in the Methods section.*
☐	☒	A description of all covariates tested
☐	☒	A description of any assumptions or corrections, such as tests of normality and adjustment for multiple comparisons
☐	☒	A full description of the statistics including central tendency (e.g. means) or other basic estimates (e.g. regression coefficient) AND variation (e.g. standard deviation) or associated estimates of uncertainty (e.g. confidence intervals)
☒	☐	For null hypothesis testing, the test statistic (e.g. *F*, *t*, *r*) with confidence intervals, effect sizes, degrees of freedom and *P* value noted *Give P values as exact values whenever suitable.*
☒	☐	For Bayesian analysis, information on the choice of priors and Markov chain Monte Carlo settings
☒	☐	For hierarchical and complex designs, identification of the appropriate level for tests and full reporting of outcomes
☒	☐	Estimates of effect sizes (e.g. Cohen's *d*, Pearson's *r*), indicating how they were calculated
☐	☒	Clearly defined error bars *State explicitly what error bars represent (e.g. SD, SE, CI)*

Our web collection on statistics for biologists may be useful.

Software and code

Policy information about availability of computer code

Data collection	No software was used.
Data analysis	TrimmomaticPE-0.36: for quality control of sequencing reads; bowtie2 version 2.1.0 by Ben Langmead (langmea@cs.jhu.edu, www.cs.jhu.edu/~langmea): for alignment; HTSeq-0.9.1: count the genes occurence; cufflinks-2.2.1 for FPKM; DESeq2 version 1.18.1: for LOG2 fold change. Correct count analysis pipeline (CoCo) (http://gitlabscottgroup.med.usherbrooke.ca/scott-group/coco): to quantify introns; R Development Core Team Version 3.3.0: for Chi-squared test; SGD server (https://www.yeastgenome.org/): for GO analyses CLC Main Workbench secondary structure analysis tool Build 1305231204: for structures; mFold (http://unafold.rna.albany.edu/?q=mfold/rna-folding-form): for structures

For manuscripts utilizing custom algorithms or software that are central to the research but not yet described in published literature, software must be made available to editors/reviewers upon request. We strongly encourage code deposition in a community repository (e.g. GitHub). See the Nature Research guidelines for submitting code & software for further information.

Data

Policy information about availability of data

All manuscripts must include a data availability statement. This statement should provide the following information, where applicable:

- Accession codes, unique identifiers, or web links for publicly available datasets
- A list of figures that have associated raw data
- A description of any restrictions on data availability

Additional data generated in this study have been submitted to the NCBI Gene Expression Omnibus (GEO; https://www.ncbi.nlm.nih.gov/geo) under the accession number GSE111056.

Field-specific reporting

Please select the best fit for your research. If you are not sure, read the appropriate sections before making your selection.

☒ Life sciences ☐ Behavioural & social sciences ☐ Ecological, evolutionary & environmental sciences

For a reference copy of the document with all sections, see nature.com/authors/policies/ReportingSummary-flat.pdf

Life sciences study design

All studies must disclose on these points even when the disclosure is negative.

Sample size	The sample size was determined by the number of introns (295) in yeast. All yeast introns were deleted and analyzed by different assays.
Data exclusions	For RT-qPCR and growth assays that were performed in at least three biological replicates and two technical replicates, the pre-established criteria for exclusion was if one data is far from the others and if this data increases the standard deviation (SD) more than 1.5 times, this data was excluded from the analyses; otherwise, all the data were kept for analyses.
Replication	The assays were performed with at least three biological replicates. All attempts at replication were successful.
Randomization	For the starvation and the nutrients depletion assay, the samples were allocated randomly in such a way that each metabolic pathway was represented in the three experimental groups.
Blinding	We analysed 295 yeast mutants. We had to keep track of the mutants used in each experiment in order to be able to analyze its outcome. Thus, blinding was not possible.

Reporting for specific materials, systems and methods

Materials & experimental systems

n/a	Involved in the study
☒	☐ Unique biological materials
☐	☒ Antibodies
☒	☐ Eukaryotic cell lines
☒	☐ Palaeontology
☒	☐ Animals and other organisms
☒	☐ Human research participants

Methods

n/a	Involved in the study
☒	☐ ChIP-seq
☒	☐ Flow cytometry
☒	☐ MRI-based neuroimaging

Antibodies

Antibodies used	Rabbit anti-RPS6, #ab40820, Abcam, lot #23 (polyclonal) Dilution 1:1000 Rabbit anti-phospho-Ser235/Ser236-S6 #2211, Cell Signaling Technology, lot GR3204358-1 (polyclonal) Dilution 1:1000 Mouse anti-PGK1 #459250, Invitrogen (now ThermoFisher Scientific), lot # F1284, clone 22C5D8 Dilution 1:10000 Donkey anti-rabbit IgG #NA934V, GE Healthcare, lot # 9451569 (peroxidase conjugate) Dilution 1:5000 Sheep anti-mouse IgG #NA931V, GE Healthcare, lot # 9597364 (peroxidase conjugate) Dilution 1:2000
Validation	All antibodies were commercially available, suitable for Saccharomyces cerevisiae and western blot as specified by the manufacturer.

Rabbit anti-RPS6 and rabbit anti-phospho-Ser235/Ser236-S6 antibodies have been used to detect total and phosphorylated S6 from Saccharomyces cerevisiae in Gonzalez et al. (2015) PLOS One. Bands of the appropriate apparent size (31 and 32 kDa) were detected and we used a deletion mutant of the Ypk3 kinase that phosphorylates S6 at Ser235 and Ser236 to control for the specificity of the anti phosho-S6 antibody.
Examples of the use of mouse anti-PGK1 used as a loading control for Western blots can be found in Petibon et al. (2016) Nucleic Acids Research. Bands of the appropriate apparent size (45 kDa) were detected.
Western blots were repeated 3 times.